PLOS PATHOGENS

RESEARCH ARTICLE

The late endosome-resident lipid bis(monoacylglycero)phosphate is a cofactor for Lassa virus fusion

Ruben M. Markosyan[1], **Mariana Marin**[2,3], **You Zhang**[2,3], **Fredric S. Cohen**[1], **Gregory B. Melikyan**[2,3]*

1 Rush University Medical Center, Department of Physiology and Biophysics, Chicago, Illinois, United States of America, **2** Department of Pediatrics, Emory University, Atlanta, Georgia, United States of America, **3** Children's Healthcare of Atlanta, Atlanta, Georgia, United States of America

* gmeliki@emory.edu

Check for updates

OPEN ACCESS

Citation: Markosyan RM, Marin M, Zhang Y, Cohen FS, Melikyan GB (2021) The late endosome-resident lipid bis(monoacylglycero)phosphate is a cofactor for Lassa virus fusion. PLoS Pathog 17(9): e1009488. https://doi.org/10.1371/journal.ppat.1009488

Editor: Juan Carlos de la Torre, The Scripps Research Institute, UNITED STATES

Received: March 16, 2021

Accepted: August 25, 2021

Published: September 7, 2021

Copyright: © 2021 Markosyan et al. This is an open access article distributed under the terms of the Creative Commons Attribution License, which permits unrestricted use, distribution, and reproduction in any medium, provided the original author and source are credited.

Data Availability Statement: All relevant data are within the manuscript and its Supporting Information files.

Funding: This work was funded by NIH R01 AI053668 to GBM The funders had no role in study design, data collection and analysis, decision to publish, or preparation of the manuscript.

Competing interests: The authors have declared that no competing interests exist.

Abstract

Arenavirus entry into host cells occurs through a low pH-dependent fusion with late endosomes that is mediated by the viral glycoprotein complex (GPC). The mechanisms of GPC-mediated membrane fusion and of virus targeting to late endosomes are not well understood. To gain insights into arenavirus fusion, we examined cell-cell fusion induced by the Old World Lassa virus (LASV) GPC complex. LASV GPC-mediated cell fusion is more efficient and occurs at higher pH with target cells expressing human LAMP1 compared to cells lacking this cognate receptor. However, human LAMP1 is not absolutely required for cell-cell fusion or LASV entry. We found that GPC-induced fusion progresses through the same lipid intermediates as fusion mediated by other viral glycoproteins–a lipid curvature-sensitive intermediate upstream of hemifusion and a hemifusion intermediate downstream of acid-dependent steps that can be arrested in the cold. Importantly, GPC-mediated fusion and LASV pseudovirus entry are specifically augmented by an anionic lipid, bis(monoacylglycero)phosphate (BMP), which is highly enriched in late endosomes. This lipid also specifically promotes cell fusion mediated by Junin virus GPC, an unrelated New World arenavirus. We show that BMP promotes late steps of LASV fusion downstream of hemifusion–the formation and enlargement of fusion pores. The BMP-dependence of post-hemifusion stages of arenavirus fusion suggests that these viruses evolved to use this lipid as a cofactor to selectively fuse with late endosomes.

Author summary

Pathogenic arenaviruses pose a serious health threat. The viral envelope glycoprotein GPC mediates attachment to host cells and drives virus entry *via* endocytosis and low pH-dependent fusion within late endosomes. Understanding the host factors and processes that are essential for arenavirus fusion may identify novel therapeutic targets. To delineate the mechanism of arenavirus entry, we examined cell-cell fusion induced by the Old World Lassa virus GPC proteins at low pH. Lassa GPC-mediated fusion was augmented

by the human LAMP1 receptor and progressed through lipid curvature-sensitive intermediates, such as hemifusion (merger of contacting leaflets of viral and cell membrane without the formation of a fusion pore). We found that most GPC-mediated fusion events were off-path hemifusion structures and that the transition from hemifusion to full fusion and fusion pore enlargement were specifically promoted by an anionic lipid, bis(monoacylglycero)phosphate, which is highly enriched in late endosomes. This lipid also specifically promotes fusion of unrelated New World Junin arenavirus. Our results imply that arenaviruses evolved to use bis(monoacylglycero)phosphate to enter cells from late endosomes.

Introduction

Old World (OW) and New World (NW) arenaviruses cause a range of diseases in humans, including severe hemorrhagic fever with high fatality rates of 15–35%. There are currently no FDA-approved vaccines or drugs to battle arenavirus infection. OW and NW arenaviruses infect a wide range of cells types *in vitro*, owing to their use of the ubiquitously expressed α-dystroglycan (α-DG) and transferrin receptor 1 (TfR1), respectively, for cell attachment and entry (reviewed in [1–3]). Binding of pathogenic Clade B NW arenaviruses to TfR1 initiates entry *via* clathrin-mediated endocytosis [3–5], whereas α-DG-driven OW arenavirus uptake occurs through a poorly characterized macropinocytosis-like pathway that is independent of clathrin, caveolin, dynamin-2, Rab5 and Rab7 [3,5–9]. Regardless of the specific receptor usage, NW and OW arenaviruses are thought to enter cells by undergoing low pH-triggered fusion with multivesicular bodies or late endosomes [2,6,8,10,11].

Fusion of arenavirus with host cells is mediated by the GP glycoprotein complex (GPC), a class I viral fusion protein [2,3,12–17]. Like many viral glycoproteins, arenavirus GPC is synthesized as an inactive GPC precursor that is cleaved at two sites, one by a signal peptidase and the other by SKI-1/S1P protease. This generates a stable signal peptide (SSP) and non-covalently associated GP1 (surface) and GP2 (transmembrane) subunits. A unique feature of the arenavirus GP complex is that the SSP remains associated with the GP2 subunit after GPC cleavage. The ~58-residue long SSP plays critical roles in GPC cleavage and transport to the plasma membrane and controls the initiation of GP conformational changes upon exposure to low pH [10,18–23].

Interestingly, arenaviruses tend to rely on more than one host factor for entry. The Lassa Fever virus (LASV) switches from α-DG to the LAMP1 receptor in acidic endosomes [24–26]. Similarly, a distant OW Lujo virus (LUJV) engages NRP-2 and CD63 at the plasma membrane and in endosomes, respectively [27]. Efficient entry of the NW Junin virus has been reported to require TfR1 and a voltage-gated calcium channel [28]. However, some arenaviruses can infect cells lacking the known receptors, albeit less efficiently [29–32]. Although LAMP1 promotes LASV entry/fusion, it is not strictly required for the GPC fusion activity [31–33]. Several lines of evidence indicate that acidic pH alone is sufficient to trigger LASV GPC conformational changes/functional inactivation [33], including GP1 dissociation from the GP2 [26] and fusion [31,33] (but see [34] reporting LASV GPC resistance to acid treatment).

The molecular mechanism for arenavirus GPC-induced membrane fusion is not well understood. Progress in delineating the mechanism of arenavirus entry/fusion in late endosomes has been impaired by lack of knowledge regarding the precise lumenal pH or composition of intracellular compartments harboring the virus. Here, we use a cell-cell fusion model to examine the pH-, receptor- and lipid-dependence of LASV GPC-mediated fusion and

characterize key intermediates of this process. We find that GPC-mediated cell-cell fusion is augmented by human LAMP1 expression and that GPC-LAMP1 binding shifts the pH optimum for fusion to a less acidic pH. We show that, similar to membrane fusion mediated by other viral proteins (e.g., [35–42]), LASV GPC-induced fusion progresses through a hemifusion intermediate and that fusion can be efficiently arrested upstream of hemifusion by incorporation of positive curvature-imposing lipids. Of note, irrespective of human LAMP1 expression, GPC-mediated fusion with the plasma membrane of a target cell appears sub-optimal, as this process tends to get stalled at a dead-end hemifusion intermediate that does not progress to a fusion pore. This finding indicates that LASV fusion may be augmented by a cofactor enriched in late endosomes. Indeed, we find that GPC-mediated membrane fusion is specifically enhanced by a late endosome-resident lipid, bis(monoacylglycero)phosphate (BMP). These findings reveal BMP as a cofactor that drives efficient LASV fusion with late endosomes.

Results

GPC mediated membrane fusion is triggered by low pH and enhanced by human LAMP1

We first examined LASV entry into cells using a luciferase reporter based single-round pseudovirus infection assay (see Materials and Methods). Human HEK293T and A549 cells were infected with HIV-1 luciferase reporter pseudoviruses bearing LASV GPC (referred to as LASVpp). Infection of both cell lines was pH-dependent, as evidenced by the abrogation of the luciferase signal in the presence of ammonium chloride that raises endosomal pH (Fig 1A, third and sixth columns). LAMP1 knock down in these two cell lines using shRNA resulted in ~2-3-fold reduction of LAMP1 expression (Fig 1B) and reduced infection (Fig 1A). The effect on infection was more pronounced in A549 cells expressing lower endogenous levels of LAMP1. In control experiments, LAMP1 knock down did not influence infection of HEK293T cells by particles pseudotyped with Influenza A virus hemagglutinin (IAVpp), but enhanced IAVpp infection of A549 cells (Fig 1A). The enhancing effect of LAMP1 knock down on IAVpp infection may be related to altered virus transport pathways and/or to changes in acidity of endosomal compartments. In agreement with the reported ability of LASV to enter cells lacking human LAMP1 in a pH-dependent manner [31,32], LASVpp infected avian QT6 cells which express a LAMP1 ortholog that is not recognized by LASV GPC [25] (Fig 1C). However, ectopic expression of human LAMP1 in these cells dramatically increased LASVpp infection without significantly affecting IAVpp infection. The above results show that LAMP1 facilitates LASV entry into cells but is not absolutely required for GPC-mediated virus fusion with acidic endosomes.

To further delineate the pH- and receptor-dependence of LASV GPC-mediated fusion, we employed a cell-cell fusion model that has been widely used for mechanistic studies of viral glycoprotein-mediated fusion (e.g., [31,39,43–48]). This model allows full control over extracellular pH and access to viral glycoproteins and cellular receptors by fusion inhibitors and antibodies throughout the fusion process. We transiently expressed LASV GPC in effector COS7 cells and brought these cells into contact with human HEK293T cells or with avian QT6 or DF1 cells expressing a LAMP1 ortholog that is not recognized by LASV [25]. Where indicated, the target cells were transfected with human LAMP1. Cell-cell fusion was triggered by exposure to an acidic buffer and the resulting fusion was assessed by fluorescence microscopy based on mixing of cytoplasmic dyes loaded into effector and target cells (illustrated in Fig 2A), as described previously [46].

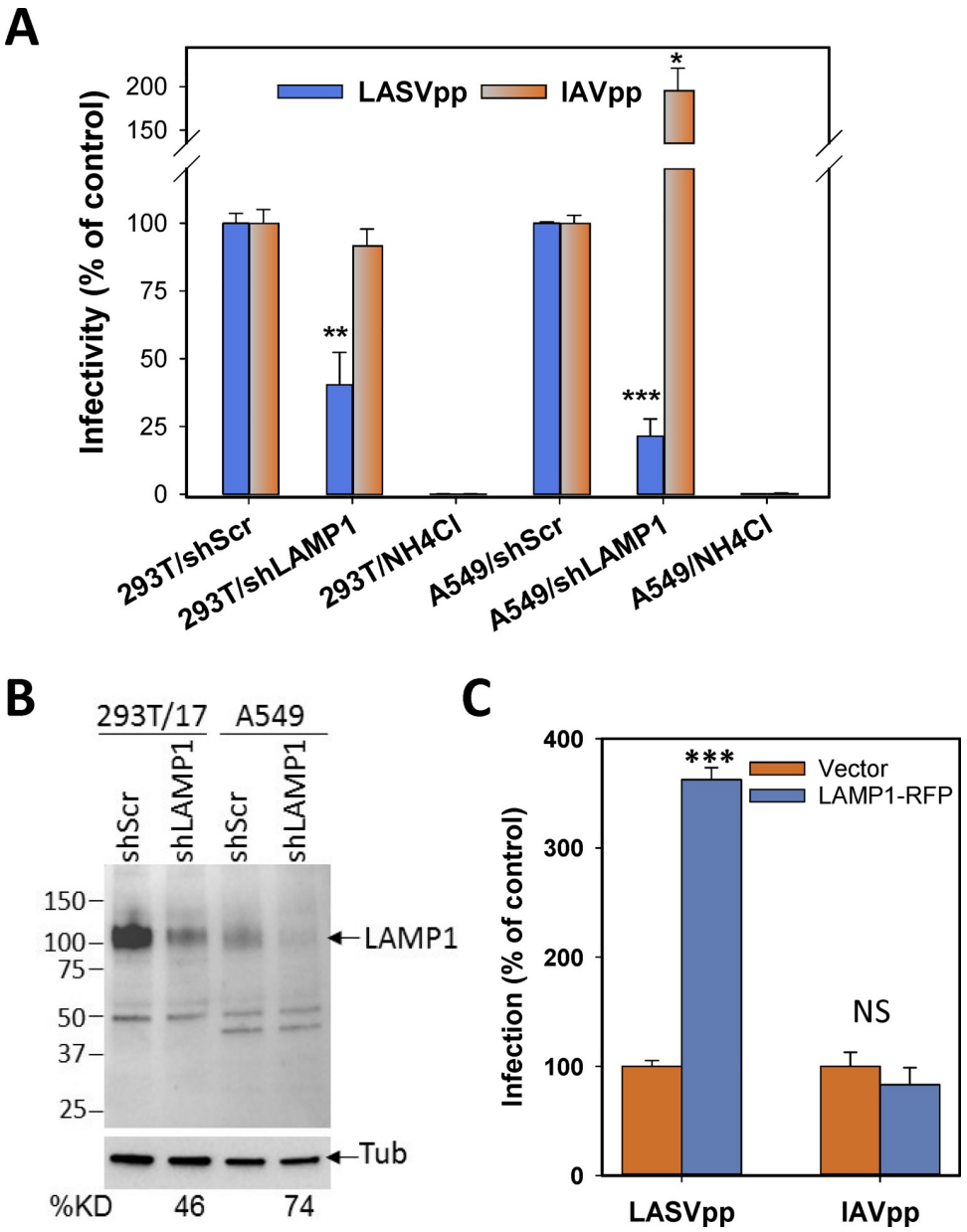

Fig 1. pH- and LAMP1-dependence of LASV pseudovirus infection. (A) Human HEK2393T or A549 cells transduced with control (shScr) or LAMP1-specific shRNA (shLAMP1) were infected with luciferase-encoding HIV-1 particles pseudotyped with LASV GPC (LASVpp) or Influenza A HA/NA glycoproteins (IAVpp). Control infections were done in the presence of 30 mM NH_4Cl to block virus entry from endosomes. The resulting luciferase signal was measured at 48 hpi and plotted as mean and SEM from three independent experiments performed in duplicate. (B) Western blot analysis of LAMP1 expression and the efficiency of shRNA knockdown in HEK293T and A549 cells. Densitometry analysis of LAMP1 expression levels relative to control cells is shown under the bottom panel. Anti-tubulin served as the loading control. (C) LASVpp infection of avian QT6 cells transfected with an empty vector or human LAMP1-mRFP encoding plasmid. Data are mean and SD for two independent experiments performed in triplicate. *, $p < 0.05$, **, $p < 0.01$, ***, $p < 0.001$, NS, not significant.

https://doi.org/10.1371/journal.ppat.1009488.g001

We initially employed suboptimal conditions–pH of 6.2 and room temperature–to trigger LASV GPC-mediated cell fusion. These conditions trigger less efficient conformational changes in GPC that is not bound to the LAMP1 receptor [33], and should thus allow better appreciation of the LAMP1-dependence of LASV fusion. The modest level of GPC-mediated

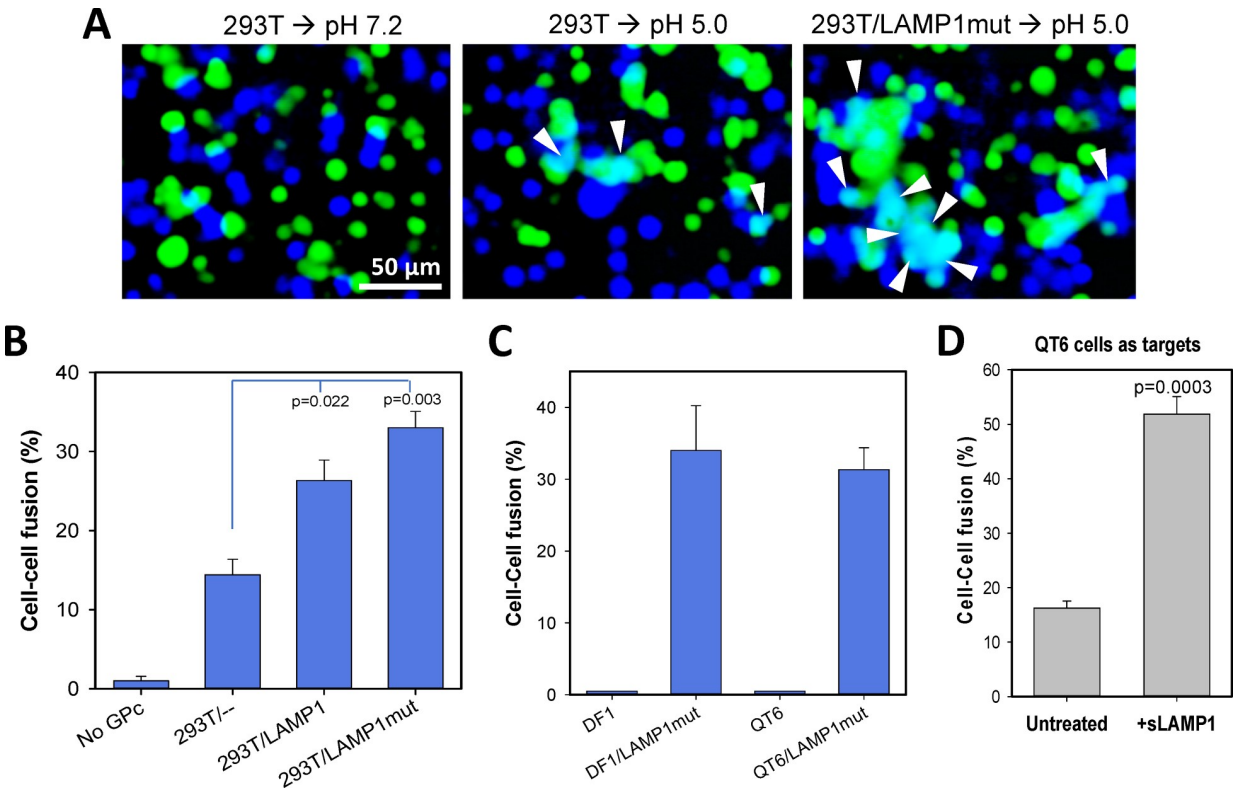

Fig 2. LAMP1-dependence of LASV GPC-mediated cell-cell fusion. (A) Representative images of effector COS7 cells transfected with LASV GPC and loaded with calcein-AM (green) and target HEK293T cells loaded with CMAC cytoplasmic dye (blue). HEK293T cells were transfected with the LAMP1 D384 mutant (LAMP1mut, right panel) or mock-transfected. Effector and target cells were mixed, allowed to adhere to poly-lysine-coated chambered slides and incubated for 30 min at room temperature. Fusion was triggered by exposing cells to a pH 5.0 buffer for 20 min at 37˚C. Control wells were exposed to a pH 7.2 buffer (left panel). Double-positive fusion products are indicated by arrowheads. Scale bar 50 μm. (B) LAMP1-dependence of fusion between LASV GPC-expressing COS7 cells (loaded with calcein-AM) and HEK293T cells (loaded with CMAC) transfected with wild-type human LAMP1, LAMP1mut or mock-transfected. As a negative control, fusion between untransfected COS7 cells with HEK293T cells was measured. A 1:1 mixture of effector and target cells was adhered to poly-lysine coated coverslips and incubated 30 min at room temperature. Cell fusion was triggered by exposure to pH 6.2 for 10 min at room temperature (suboptimal trigger), and the fraction of cells positive for both cytoplasmic markers was measured after an additional incubation for 1 h at 37˚C, neutral pH. The results are means and SEM from three independent experiments. (C) LAMP1-dependence of GPC-mediated fusion with avian DF-1 and QT6 cells. Avian cells transfected or not transfected with the human LAMP1mut were brought in contact with LASV GPC-expressing COS7 cells and exposed to pH 5.0 for 10 min at room temperature. The results are means and SEM from three independent experiments. (D) Soluble LAMP1 (sLAMP1) enhances GPC-mediated fusion with QT6 cells. GPC-expressing COS7 cells were co-plated with QT6 cells on coverslips for 30 min at room temperature to allow attachment and cell-cell contacts. The cells were further incubated in the absence or in the presence of 0.05 μg/ml of sLAMP1 for 20 min at room temperature, and fusion was triggered under optimal conditions (pH 5.0 at 37˚C, 20 min). The results are means and SEM from three independent experiments.

https://doi.org/10.1371/journal.ppat.1009488.g002

fusion with HEK293T cells under these suboptimal conditions (Fig 2B) is in accord with a fraction of the endosome/lysosome-resident LAMP1 receptor expressed on the cell surface [49]. Overexpression of human LAMP1 or the LAMP1 D384 mutant (hereafter referred to as LAMP1mut) increased the cell surface level of this receptor (S1 Fig) and enhanced LASV GPC-mediated cell fusion (Fig 2A and 2B). (LAMP1mut lacks an endocytic signal contributing to better expression at the plasma membrane [25]). The observed mixing of two cytoplasmic markers was specifically induced by LASV GPC, since mock-transfected COS7 cells failed to fuse with target cells (Fig 2B), and the arenavirus-specific inhibitor ST-193 suppressed fusion in a dose-dependent manner (S2A Fig).

Previous studies [31,32] and our infectivity data (Fig 1C) suggest that LAMP1 is not absolutely required for LASV fusion. To confirm the ability of LASV to undergo

LAMP1-independent fusion, we fused GPC-expressing cells with avian DF-1 or QT6 cells expressing a LAMP1 ortholog that is not recognized by LASV [25]. Whereas background levels of LASV GPC-mediated fusion with avian DF-1 or QT6 cells were detected under sub-optimal conditions (pH 5.0, room temperature, Fig 2C), significant fusion with these target cells was observed under optimal conditions (pH 5.0, 37˚C, Fig 2D). Ectopic expression of LAMP1mut in avian cells permitted highly efficient fusion (Fig 2C and 2D). Lassa GPC-mediated fusion with QT6 cells was also markedly enhanced by addition of a soluble recombinant human LAMP1 (sLAMP1) (Fig 2D). The above results show that, while not absolutely required for LASV GPC-mediated fusion, human LAMP1 markedly increases fusion efficiency.

GPC-LAMP1 interaction allows LASV fusion at higher pH

We assessed the pH-dependence of LASV fusion by exposing the effector/HEK293T cell complexes to buffers of different acidity. A pH threshold of LASV GPC-mediated cell fusion was ~6.2, with maximal fusion at pH 4.8 (Fig 3A), in general agreement with previous studies [10,31]. Ectopic expression of LAMP1mut in target cells increased the overall efficiency of fusion without significantly affecting the shape of the curve (Fig 3A). The modest reduction in fusion efficiency at pH<4.8 may be caused by acid-mediated GPC inactivation known to occur at pH $\leq$ 4.0 in the absence of a target cell (S2B Fig and [26,33]). Parallel experiments with avian QT6 cells lacking human LAMP1 revealed that ectopic expression of human LAMP1mut increased GPC-mediated fusion (Fig 3B). The LAMP1mut effect was the most pronounced at mildly acidic pH, consistent with reports that LAMP1 binding shifts the pH optimum of GPC-mediated fusion to higher values [25,31,33]. A quasi-linear pH-dependence of fusion with both QT6 and QT6/LAMP1mut cells at pH below ~6.0 suggests that fusion is predominantly acid-dependent, but receptor-independent in this pH range. The difference between the pH-dependence of fusion with HEK/293T and QT6 cells is surprising and might indicate that cell type- or species-specific factors other than LAMP1 may promote LASV GPC refolding at acidic pH.

LASV fusion is reversibly arrested by positive-curvature lipids

Diverse membrane fusion reactions can be blocked by exogenous lyso-lipids that confer positive curvature to the contacting membrane leaflets and thereby disfavor the formation of a net negative curvature stalk structure (Fig 4A and [50–52]). This lipid-arrested stage (LAS) is largely reversible upon washing away lysolipids and commences at neutral pH [44,53], implying that the viral proteins are arrested in a "committed" stage that is downstream of low pH-dependent steps. Like other protein-mediated fusion reactions, LASV GPC-mediated fusion was blocked when lyso-PC was present before and during a low pH pulse, but fusion ensued upon removal (at neutral pH) of this lipid (Fig 4B). This result implies that LASV fusion progresses through curved lipid intermediates of net negative curvature, likely a stalk and a hemifusion diaphragm.

LASV fusion progresses through a hemifusion intermediate that can be arrested at low temperature

Membrane fusion mediated by diverse viral glycoproteins progresses through a common hemifusion intermediate (reviewed in [54–56]) (Fig 4A). This intermediate is formed through merger of the contacting leaflets of two membranes, while distal leaflets form a new bilayer referred to as hemifusion diaphragm [57,58] (Fig 4A). It has been shown that low pH-triggered viral fusion can be arrested at a local hemifusion stage in the cold (referred to as cold-arrested stage, CAS) [46,53,59–61] (Fig 4A). After creating CAS, fusion can be recovered at neutral pH

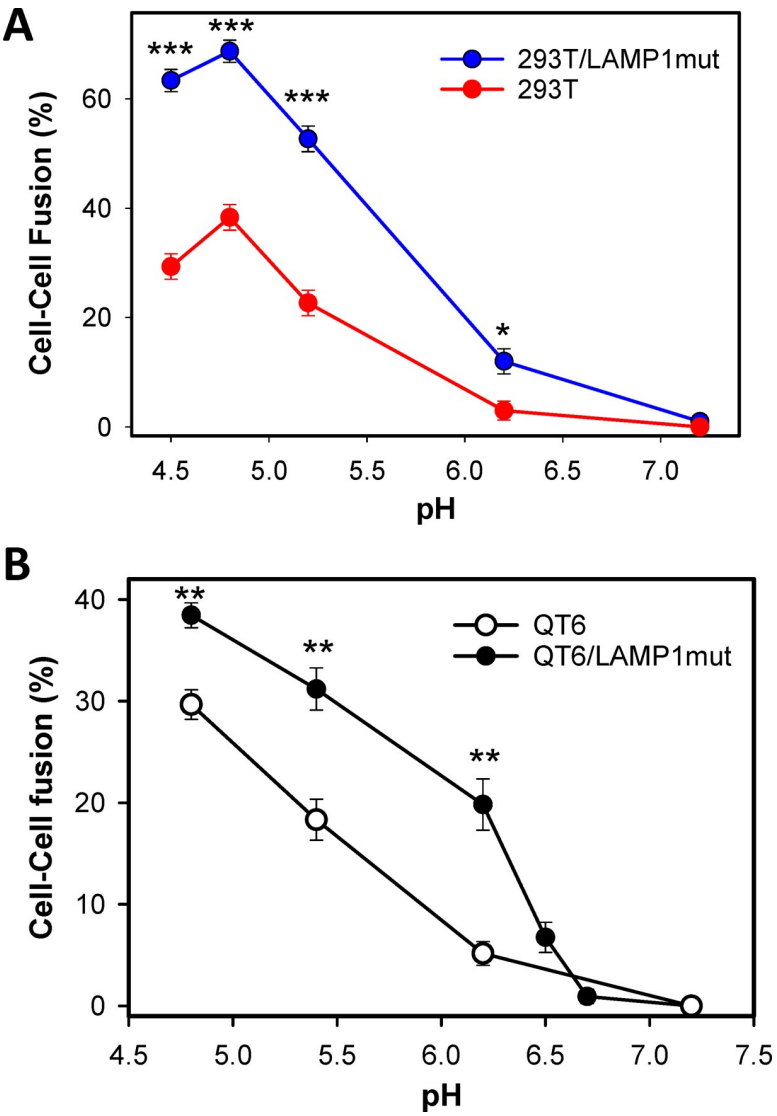

Fig 3. pH-dependence of LASV GPC-mediated cell-cell fusion. (A) Fusion between COS7 cells transfected with LASV GPC and HEK293T cells mock-transfected or transfected with LAMP1mut was triggered by exposure to buffers of different acidity for 20 min at 37˚C (optimal trigger). The results are means and SEM from three independent experiments. (B) pH-dependence of fusion, using the protocol described in panel A, was measured between LASV GPC-expressing COS7 cells and plain QT6 cells or QT6 cells transfected with LAMP1mut. The results are means and SEM from three independent experiments. *, $p<0.05$; **, $p<0.01$, ***, $p<0.001$.

https://doi.org/10.1371/journal.ppat.1009488.g003

by raising temperature. In other words, steps of fusion downstream of CAS are temperature-dependent but no longer require low pH. The formation of a hemifusion intermediate, including the one formed at CAS, can be indirectly inferred by treating cells with chlorpromazine (CPZ) at neutral pH, which selectively destabilizes a hemifusion diaphragm and promotes full fusion [57] (Fig 4A).

We first asked if LASV GPC-mediated fusion exhibits a natural tendency to get stuck at a hemifusion stage, as is the case for membrane fusion mediated by other low pH-dependent viruses, especially when suboptimal triggers for fusion (insufficiently low pH and/or reduced temperature) are employed [44,53,61]. We found that GPC-mediated fusion triggered under suboptimal conditions (pH 6.2, room temperature) was markedly enhanced by a brief

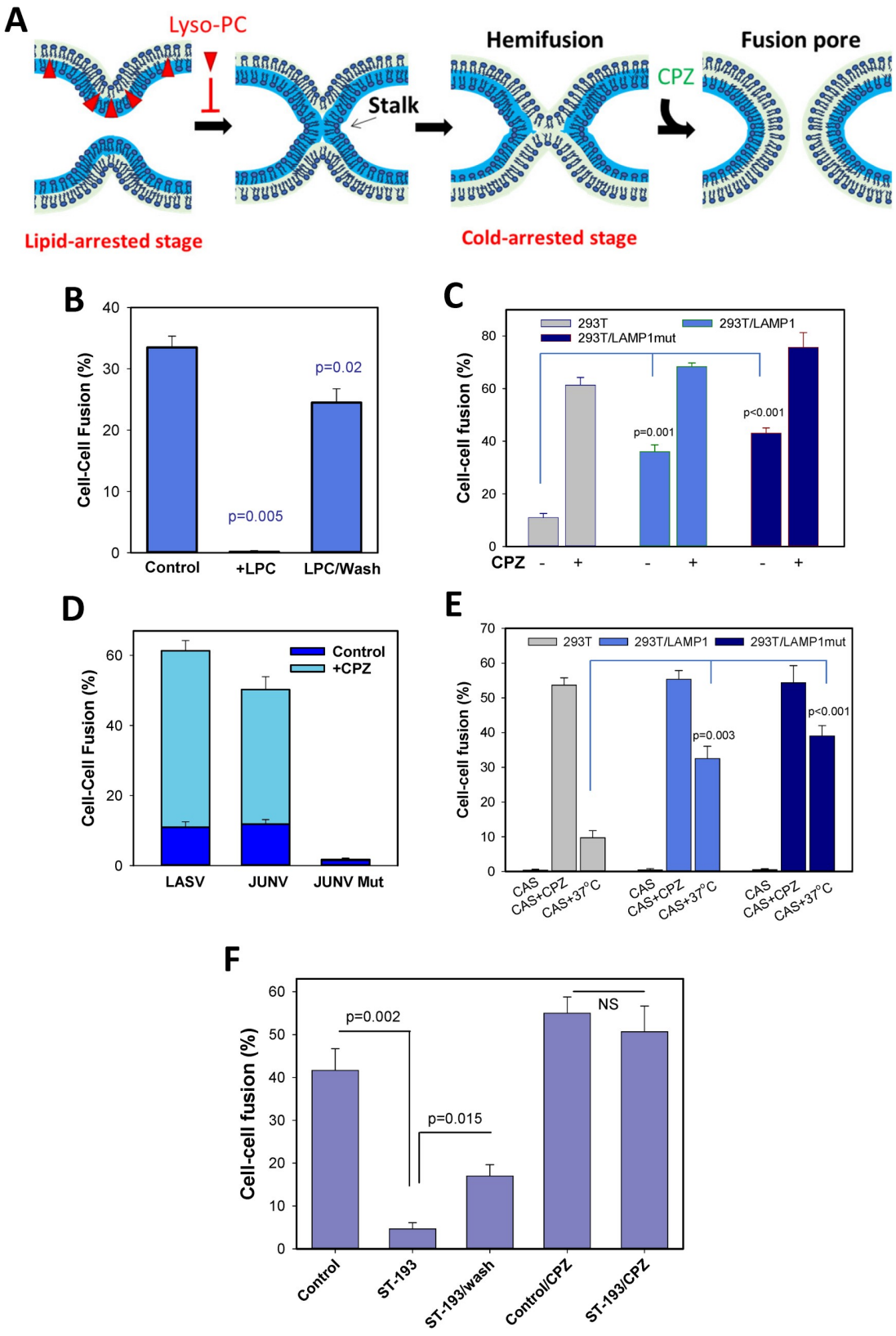

Fig 4. LASV GPC-mediated fusion progresses through a hemifusion intermediate that is blocked by lyso-lipids. (A) Illustration of cold-arrested (CAS, hemifusion) and lyso-lipid-arrested (LAS, pre-hemifusion) intermediates and the effect of

chlorpromazine (CPZ). (B) Lipid-arrested stage of LASV fusion. GPC-expressing COS7 cells were bound to QT6 cells transfected with LAMP1mut in the presence of 285 μM stearoyl lyso-PC for 30 min at room temperature, followed by exposure to pH 5.0 at room temperature in the presence of lyso-PC. Cells were either washed with delipidated BSA (2 mg/ml) to remove lyso-PC (right bar) or left with lyso-PC (middle bar) and incubated for 30 min at 37˚C. The results are means and SEM from three independent experiments. (C) The effect of CPZ on fusion between GPC-expressing COS7 cells and HEK293T cells mock-transfected or transfected with LAMP1 or LAMP1mut. Cell fusion was triggered under sub-optimal conditions (pH 6.2, 10 min at room temperature). After an additional 1 h incubation at 37˚C, cells were treated with CPZ (0.5 mM) for 1 min or left untreated. The results are means and SEM from three independent experiments. (D) CPZ enhances LASV and Junin GPC-mediated cell fusion. Fusion between LASV or Junin GPC-expressing COS7 cells and HEK293T cells was triggered by exposure to pH 6.2 (for LASV) or pH 5.5 (JUNV). After a 20 min incubation at 37˚C, cells were treated for 1 min with 0.5 mM CPZ at room temperature (n = 3). (E) Cold-arrested intermediate (CAS) of LASV GPC fusion. GPC-expressing COS7 cells were incubated with HEK293T cells (transfected or not with LAMP1 or LAMP1mut) for 30 min at room temperature and exposed to pH 6.2 on ice for 10 min. Cells were either immediately treated with cold 0.5 mM CPZ for 1 min or additionally incubated for 1 h at 37˚C, neutral pH. The results are means and SEM from three independent experiments. (F) ST-193 captures LASV fusion at a hemifusion intermediate. COS7 cells expressing LASV GPC were mixed with HEK293T cells, attached to glass slides and allowed to adhere and form contacts for 30 min at room temperature. Fusion was initiated by exposure to pH 5.0 for 15 min at 37˚C, in the presence or absence of 150 μM ST-193. Cells were either washed to remove the inhibitor or kept in the presence of ST-193, and either immediately treated with 0.5 mM CPZ for 1 min or further incubated at neutral pH for 1 h, 37˚C. The results are means and SEM from three independent experiments.

https://doi.org/10.1371/journal.ppat.1009488.g004

exposure to CPZ after returning to neutral pH (Fig 4C). This CPZ-mediated fusion enhancement was much more pronounced for plain HEK293T cells (>6-fold), as compared to cells expressing wild-type or mutant LAMP1 (~2-fold, Fig 4C). Notably, over-expression of LAMP1 markedly decreased the fraction of dead-end hemifusion structures that did not naturally progress to full fusion. Higher levels of ectopically expressed LAMP1 on the cell surface did not considerably increase the overall efficiency of formation of hemifusion sites (i.e., CPZ-sensitive lipid intermediates), but markedly enhanced the probability of transition to full fusion at 37˚C. A similar dramatic increase in cell-cell fusion was observed after treatment of Junin virus GPC-mediated cell fusion products with CPZ, whereas this treatment was without effect in control experiments using cells expressing a fusion-incompetent GPC mutant [20] (Fig 4D). Thus, under suboptimal conditions, GPC tends to create hemifusion structures that do not resolve into full fusion, and the formation of such dead-end intermediates is independent of the LAMP1 expression level; these dead-end hemifusion structures can be converted to full fusion by CPZ treatment.

Next, we tested the possibility of capturing LASV fusion at a cold-arrested stage (CAS, Fig 4A) by exposing effector/target cell pairs to low pH in the cold. A reversible arrest of GPC-mediated cell-cell fusion at CAS was evident by the commencement of fusion after shifting to 37˚C at neutral pH (Fig 4E). As observed for uninterrupted LASV GPC-mediated cell-cell fusion (Fig 2), ectopic expression of LAMP1 or LAMP1mut markedly enhanced the extent of fusion after shifting cells captured at CAS to 37˚C (Fig 4E). Importantly, CPZ treatment of cells arrested at CAS (after returning to neutral pH, still at low temperature) promoted efficient fusion (Fig 4E), consistent with the formation of local hemifusion structures at CAS. In control experiments, CPZ treatment did not promote fusion of effector/target cell pairs that were not exposed to low pH or cells expressing a fusion-defective GPC mutant after exposure to low pH (e.g., Fig 4D). CPZ treatment induced more fusion between cells captured at CAS than a shift to 37˚C and this difference was more apparent for fusion with suboptimal target cells (Fig 4E). These results show that GPC-LAMP1 interactions increase the probability of conversion of hemifusion to full fusion.

Arenavirus fusion inhibitor captures LASV GPC-induced fusion at a hemifusion stage

The small-molecule arenavirus fusion inhibitor ST-193 has been shown to block pH-induced conformational changes in GPC, including the shedding of the GP1 subunit, but the fusion

block can be overcome at sufficiently acidic pH [62]. ST-193 is thought to act by binding to the interface between the GP2 subunit transmembrane domain and the stable signal peptide [62], thereby disfavoring the early steps of GPC refolding at low pH. Since, the compound appears to interfere with pH-induced GPC refolding, we asked whether ST-193 blocks LASV fusion at early steps prior to membrane merger. Effector-target cell complexes were exposed to pH 5.0 at 37˚C in the presence of a high concentration of ST-193 that almost completely inhibits cell-cell fusion (Figs 4F and S2A). Subsequent removal of the inhibitor at neutral pH resulted in only a partial recovery of fusion (Fig 4F), indicating that a large fraction of GPC proteins underwent irreversible conformational changes and inactivated at low pH in the presence of ST-193. Importantly, CPZ application immediately after removal of ST-193 and in control samples not exposed to ST-193 induced efficient fusion that exceeded the level of uninterrupted fusion at 37˚C (Fig 4F). These findings show that, in the presence of ST-193, GPC undergoes low pH-dependent conformational changes that promote dead-end hemifusion. Similar levels of CPZ-mediated fusion for control and ST-193 treated samples (Fig 4F) suggest that the initial acid-dependent steps of GPC-mediated membrane fusion are not noticeably affected by this inhibitor when cells are subjected to an optimal trigger. Dead-end hemifusion structures formed in the presence of ST-193 are effectively converted to full fusion by CPZ treatment, while less than 30% of hemifusion structures naturally resolve into full fusion at 37˚C (Fig 4F).

Late steps of LASV GPC-mediated fusion are enhanced by a late endosome-resident lipid

LASV is thought to fuse with multivesicular bodies/late endosomes [2,3,6,8]. However, LASV GPC can mediate fusion with LAMP1-expressing cells at mildly acidic pH typical for early endosomes (Fig 3 and [31–33]). We therefore asked if LASV entry from early endosomes may be delayed due to the need for an additional host factor localized to late endosomes. The unusual anionic lipid, bis(monoacylglycero)phosphate (BMP), also known as lysobisphosphatidic acid, is greatly enriched in late endosomes (around 15% of the total lipids [63,64]).

It has been reported that preincubation of cells with anti-BMP antibodies diminishes LASV infection [6]. We have now found that preincubation with anti-BMP antibody modestly inhibited LASVpp fusion and, to a lesser degree, IAVpp fusion, whereas pretreatment with control isotype antibodies was without effect (S3 Fig). The modest effect on IAVpp fusion may be related to disruption of biogenesis of multivesicular bodies and/or of cholesterol transport [65–68]: prolonged incubation with anti-BMP antibodies is known to disrupt several essential cellular processes, including cholesterol transport and biogenesis of multivesicular bodies [65–68]. These pleotropic effects may indirectly disfavor LASV fusion by disrupting virus uptake and/or transport to permissive intracellular compartments. In this regard, cell-cell fusion appears well-suited for exploring lipid-dependence of LASV GPC-mediated fusion.

To directly investigate the effect of lipids on LASV fusion, the effector/target cell complexes were pretreated with BMP or zwitterionic lipid DOPC (control) prior to exposure to low pH. We observed specific promotion of LASV GPC-mediated cell fusion by exogenous BMP, but not by DOPC (Fig 5A). This enhancing effect of BMP was observed across the range of LAMP1 expression, using plain HEK293T cells and cells transfected with LAMP1 or LAMP1-mut (Fig 5A). Also, BMP, but not another anionic lipid, DOPS, markedly enhanced GPC-mediated fusion with suboptimal QT6 cells (Fig 5B). This finding shows that non-specific electrostatic interactions are not responsible for the observed enhancement of LASV fusion by BMP. BMP also enhanced the Junin virus GPC-mediated cell fusion by ~4-fold, whereas DOPC and DOPS were without effect (Fig 5C). In contrast, influenza HA-mediated fusion

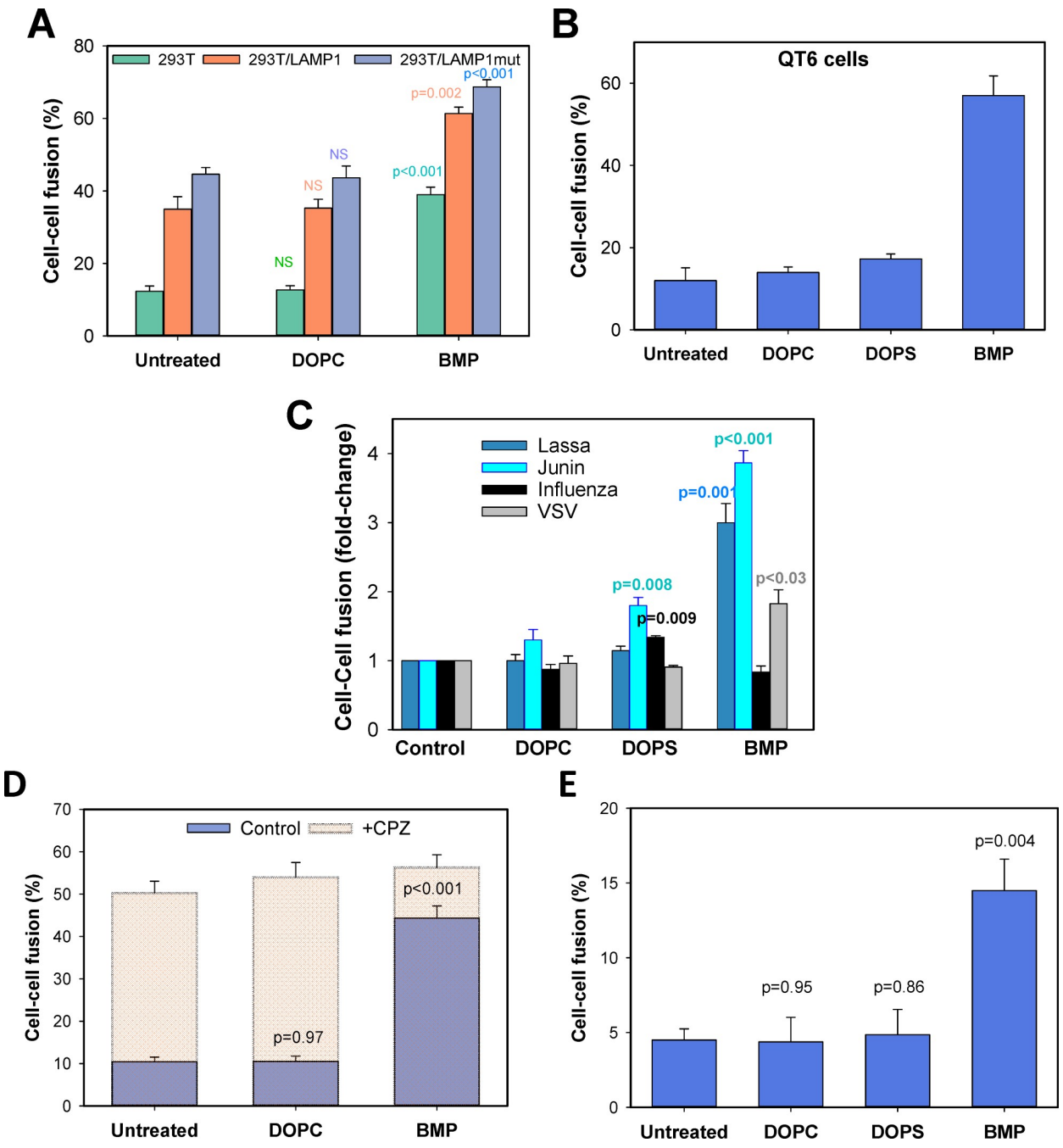

Fig 5. Lipid-dependence of LASV GPC-mediated cell fusion. (A) COS7 cells transiently expressing LASV GPC were co-incubated with mock-transfected or LAMP1 or LAMP1mut transected 293T cells in the presence of 10 μg/ml DOPC or BMP dissolved in BSA (1 mg/ml) for 20 min at room temperature. Cell fusion was triggered by exposure to pH 6.2 at room temperature in the absence of exogenous lipids and was measured after an additional incubation for 1 h at 37˚C. The results are means and SEM from three independent experiments. (B) GPC-expressing COS7 cells were incubated with QT6 cells in the presence of 10 μg/ml DOPC, DOPS or BMP dissolved in BSA (1 mg/ml) for 20 min at room temperature. Cell fusion was triggered by exposure to pH 5.0 at 37˚C for 20 min in the absence of exogenous lipids. The results are means and SEM from three independent experiments. (C) COS7 cells expressing LASV or Junin Virus GPC or IAV HA were brought in contact with HEK293T cells, incubated with 10 μg/ml DOPC, DOPS or BMP dissolved in BSA for 20 min at room temperature and exposed to pH 5.0 for 20 min at 37˚C. The results are means and SEM from four independent experiments. (D) BMP facilitates transition from hemifusion to fusion. COS7 cells expressing LASV GPC were incubated with HEK293T cells in the presence of 10 μg/ml DOPC or BMP dissolved in BSA (1 mg/ml) for 20 min at room temperature. Cell fusion was initiated by exposure to pH 6.2 for 10 min at room temperature in the absence of lipids followed by incubation at 37˚C for 1 h. followed by a brief (1 min) exposure to 0.5 mM CPZ or to PBS (control). The results are means and SEM from three independent experiments. (E) Lipid-dependence of transition from cold-arrested stage (CAS) to full fusion. Fusion between LASV GPC-expressing COS7 cells

and QT6 cells was initiated by exposure to pH 5.0 for 10 min at 4˚C followed by treatment with 10 μg/ml of indicated lipids in BSA for 10 min at room temperature, at neutral pH, and an additional 30 min-incubation at 37˚C.

https://doi.org/10.1371/journal.ppat.1009488.g005

was not affected by either BMP or DOPC but was modestly promoted by DOPS. In agreement with the published work on the lipid-dependence of Vesicular Stomatitis Virus (VSV) fusion [69], VSV G protein-mediated cell fusion was modestly augmented by BMP, but not by DOPC or DOPS treatment (Fig 5C). Note that failure of exogenous DOPS to promote cell-cell fusion mediated by GPC was not due to the lack of incorporation into the plasma membrane, as revealed by staining cells with Annexin V (S4A Fig).

BMP promotes the formation and growth of GPC-mediated fusion pores

To further delineate the role of BMP in GPC-mediated fusion, we asked whether its effect is dependent on incorporation of this lipid into a target vs. GPC-expressing cells. Effector or target cells detached from culture dishes were separately treated with DOPC or BMP, mixed and exposed to low pH. In control experiments, a mixture of effector and target cells was pretreated with the indicated lipids. As shown in S4B Fig, addition of BMP increased the efficiency of GPC-mediated cell fusion by ~2.5-fold compared to DOPC control, irrespective of whether BMP was incorporated into effector or target cells. Promotion of LASV fusion upon BMP incorporation into effector cells is expected if it affects late, post-hemifusion steps of fusion; merged contacting leaflets of two membranes will allow BMP redistribution from one membrane to another at the potential fusion site.

To determine whether BMP augments late stages of GPC-mediated fusion downstream of pH-independent steps, we employed two strategies. First, the products of GPC-mediated fusion of cells pretreated with BMP or DOPC or left untreated (negative controls) were briefly exposed to CPZ to fully fuse cells arrested at hemifusion. The increase in fusion was dramatic for untreated or DOPC-pretreated cells, but modest for BMP-pretreated cells which had largely fused prior to addition of CPZ (Fig 5D). The extent of fusion after CPZ addition was independent of pretreatment. These results suggest that the efficiency of formation of CPZ-sensitive hemifusion structures is independent of BMP, whereas the probability of conversion of these intermediates to full fusion is dramatically and specifically increased by BMP. The second strategy was to capture cell-cell fusion at CAS, add various lipids, at neutral pH, and then raise temperature. Fusion was potently promoted by the addition of BMP at CAS, but not by the addition of DOPC or DOPS (Fig 5E).

Finally, we examined the effect of exogenously added BMP on the size of GPC-mediated fusion pores and their propensity to enlarge. Toward this goal, we performed time-lapse imaging of the redistribution of a small cytoplasmic marker, calcein, between effector and target cells (Fig 6A and 6B) and deduced the pore permeability from the rate of dye redistribution, as described previously [70,71]. Interestingly, GPC-mediated redistribution of calcein between the dye donor and acceptor cell pairs was much slower than for cell-cell fusion mediated by other viral glycoproteins [43,70]). Moreover, calcein redistribution often stalled after a few minutes so that the dye did not fully equilibrate between the two cells (Fig 6A and 6B). This result suggests that any GPC-mediated fusion pores that do form remain small under our experimental conditions and even tend to close. The average pore permeability profile confirmed the failure of GPC-mediated fusion pores to grow (Fig 6E). In stark contrast, fusion pores formed between BMP-pretreated cells grew efficiently, as evidenced by a quick and complete redistribution of calcein (Fig 6C, 6D and 6E). Control experiments showed no significant effect of DOPC on the initial size or enlargement of GPC-mediated fusion pores (Fig 6E). We also measured the kinetics of fusion pore formation based on the onset of calcein

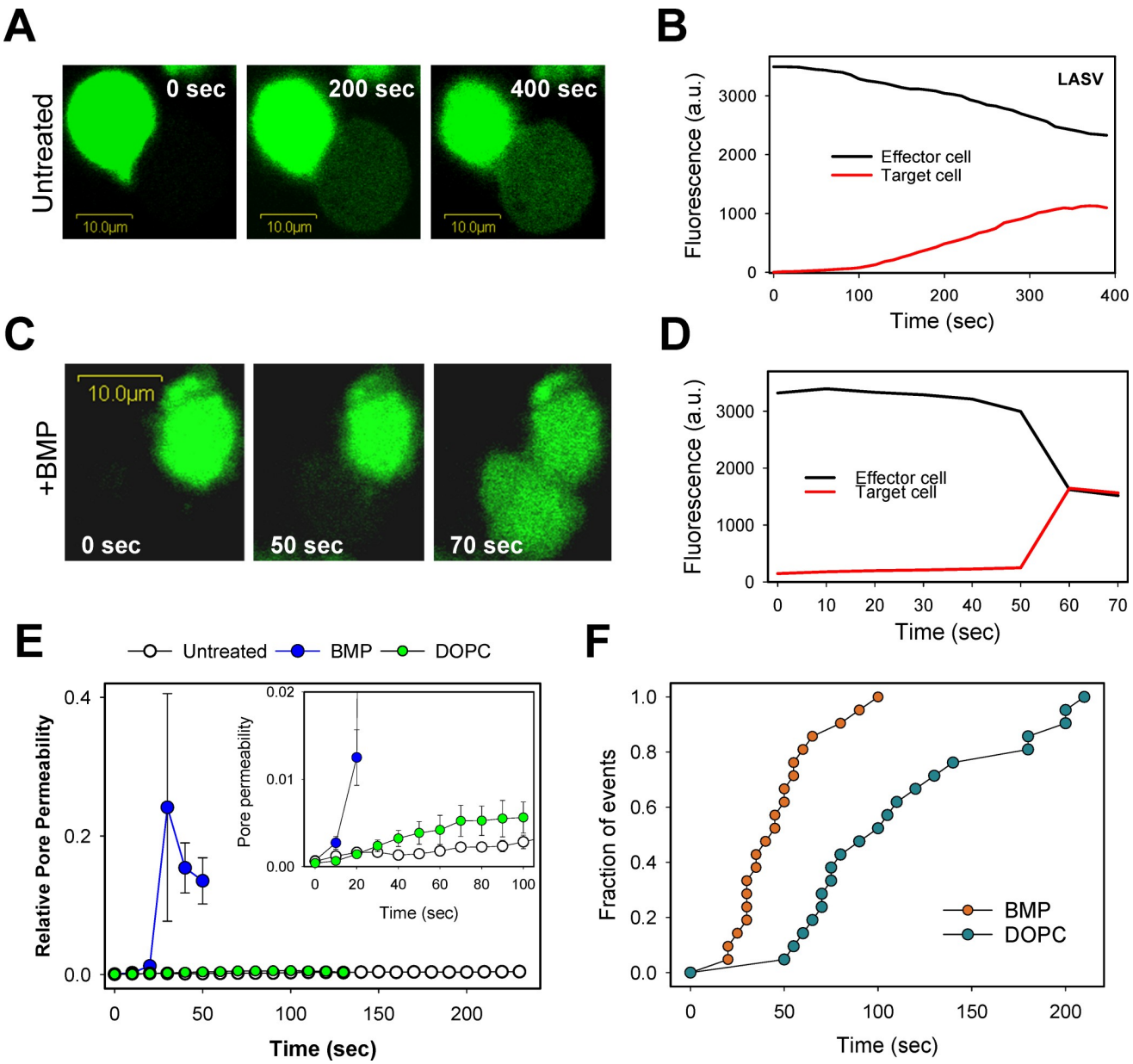

Fig 6. BMP markedly promotes the formation and enlargement of LASV GPC-mediated fusion pores. Effector COS7 cells expressing GPC were loaded with calcein (green), mixed with unlabeled 293T cells and adhered to poly-lysine coated coverslips. Cells were then pre-treated with 20 μg/ml of BMP or DOPC for 10 min at room temperature or left untreated. Cell-cell fusion was triggered by transferring cells to a pH 5.0 buffer and quickly raising the temperature to 37˚C through an IR temperature jump protocol (see Materials and Methods). (A, B) Snapshots and fluorescence intensities showing partial calcein redistribution between untreated effector and target (dye donor and acceptor) cells. (C, D) Same as in panels A, B, but for cells pretreated with BMP. (E) Ensemble average of permeabilities of six fusion pores for untreated and DOPC- or BMP-treated cells. Individual pore permeability traces calculated as described in Materials and Methods were aligned so that t = 0 represents a time point immediately before dye redistribution was detected. *Inset*: Initial permeability profiles of fusion pores. Error bars are SEM. (F) Kinetics of fusion pore formation for control and BMP-treated cells. The data points represent time after raising the temperature until the onset of calcein transfer.

https://doi.org/10.1371/journal.ppat.1009488.g006

redistribution and found that BMP pretreatment markedly accelerated the rate of cell-cell fusion (Fig 6F). Collectively, the above results show that BMP selectively enhances post-hemifusion steps of LASV fusion, including the formation and dilation of fusion pores.

Excessive accumulation of BMP in late endosomes promotes LASV fusion and infection

In contrast to the effect of BMP on cell-cell fusion, a direct LASV pseudovirus-cell fusion assay based on a beta-lactamase reporter [72] did not reveal a significant effect of this or other lipids (S5 Fig). A possible reason for the lack of BMP effect on viral fusion is that late endosomes already contain high levels of this lipid and thus support optimal LASVpp fusion. Alternatively, exogenously added BMP may not be sorted to intracellular compartments used by LASV for entry. We therefore probed the lipid-dependence of LASVpp fusion by forcing virus fusion with the plasma membrane, which does not contain detectable levels of BMP [73]. LASVpp were pre-bound to cells, and viral fusion was triggered by exposure to low pH in the presence of Bafilomycin A1, which blocks the conventional route of virus infection by raising endosomal pH. Pretreatment of virus-cell complexes with BMP, but not DOPC or DOPS, significantly increased the extent of forced LASVpp fusion with the plasma membrane (S5E Fig). By contrast, forced virus-cell fusion mediated by the IAV HA glycoprotein was not affected by BMP. These results suggest that arenavirus GPC-mediated membrane fusion is specifically promoted by BMP and that this lipid-dependence may favor LASV entry from late endosomes.

Since our attempts to increase levels of functionally relevant BMP by exogenous addition of this lipid were unsuccessful, we took advantage of the link between BMP and cholesterol transport from these compartments [65,66,73,74]. It has been demonstrated to interference with BMP functions results in excessive accumulation of cholesterol in late endosomes and, conversely, accumulation of cholesterol correlates with increased levels of BMP [74]. We therefore compared LASVpp fusion and the levels of cholesterol and BMP in parental CHO cells and cells expressing an NPC1 mutant defective in cholesterol transport (referred to as CHO.NPC1mut cells, [75]). Since excessive cholesterol accumulation in late endosomes has been documented in CHO.NPC1mut cells [75], we reasoned that these cells would also exhibit elevated levels of BMP. Indeed, staining these cells for cholesterol, using filipin, and for BMP, using anti-BMP antibodies, revealed elevated cholesterol and BMP levels (~2-fold) in the perinuclear region of CHO.NPC1mut cells as compared to CHO cells (Fig 7A and 7B). Importantly, LASVpp fusion with CHO.NPC1mut cells was markedly enhanced compared to CHO cells (Fig 7C). In control experiments, fusion of particles pseudotyped with EBOV GP (EBOVpp) that uses NPC1 as the receptor [76,77] was abrogated, IAVpp fusion was modestly enhanced, while VSVpp fusion was not affected by the NPC1 mutation (Fig 7C). These results support the role of BMP in promoting LASV fusion with late endosomes.

Discussion

Here, using single-cycle infectivity and cell-cell fusion assays, we show that, in agreement with published work [25,31,32], LASV GPC-mediated fusion is triggered by low pH and augmented by interaction with human LAMP1. Further, we find that, like fusion mediated by other viral proteins, LASV GPC-induced fusion progresses through highly curved lipid intermediates–stalk and a downstream hemifusion structure that are strongly modulated by the lipid composition of the fusing membranes. However, in spite of common features shared with other viral fusion proteins, arenavirus GPC-mediated fusion exhibits several unique properties: (1) resistance to restriction by interferon-induced transmembrane proteins (IFITMs) [35,78,79]; (2) GPC-mediated permeabilization of the viral membrane prior to fusion [78]; and (3) dependence on BMP for efficient fusion (Figs 5–7).

We also show that LASV GPC-mediated fusion with avian cells exhibits an unusually shallow pH-dependence and that human LAMP1 expression enhances fusion at mildly acidic pH

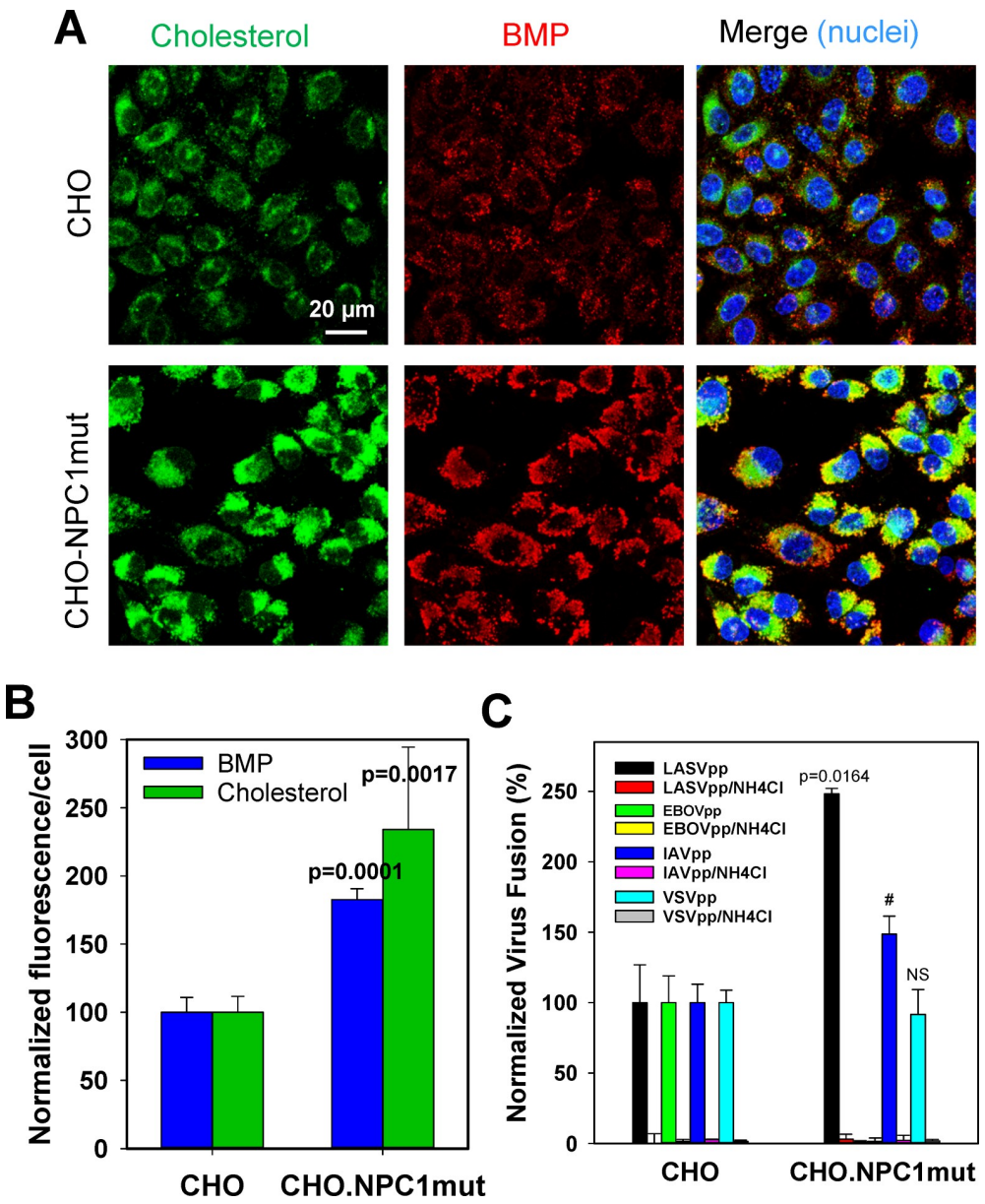

Fig 7. Increased intracellular levels of BMP promote fusion of LASV pseudoviruses. (A) Images of CHO and CHO.NPC1mut cells permeabilized and stained for cholesterol with filipin and for BMP with anti-BMP antibody. Cell nuclei were stained with far-red dye. (B) Quantification of the levels of cholesterol and BMP based on fluorescence intensity per cell after background subtraction. 6 fields of view, each containing ~30 cells were analyzed. (C) Fusion activity of LASVpp, EBOVpp, IAVpp and VSVpp in CHO and CHO.NPC1mut cells measured by a BlaM assay. As negative controls, fusion experiments were carried out in the presence of 40 mM NH_4Cl. Data are means and SD of two independent experiments performed in triplicate. NS, not significant. (# denotes that, although promotion of IAVpp fusion did not reach significance due to variation between independent experiments, enhancement of IAV fusion was significant in each experiment performed in triplicate).

https://doi.org/10.1371/journal.ppat.1009488.g007

(Fig 3B). This pH-dependence contrasts with the steep pH-dependencies of other viral fusion reactions (e.g., [44, 80]). Perhaps, acid-induced conformational changes in GPC at mildly acidic pH occur in a less cooperative manner in the absence of human LAMP1. Consistent with the ability of low pH to induce refolding of LASV GPC, exposure to pH 4.0 in the absence of target cells leads to conformational changes and GP1 shedding from GP2 [25,33], resulting

in functional inactivation of this protein (S2 Fig and [33]). This feature of LASV fusion is in contrast with Avian Sarcoma and Leukosis Virus Env glycoprotein, which becomes responsive to low pH and can mediate membrane fusion only after binding to a cognate receptor [44,81]. We note that, although our finding that LASV fusion can occur at mildly acidic pH is in general agreement with other reports [22,31,33], a few studies have reported a considerably lower pH range for GPC-mediated cell-cell fusion [34,82]. The reason for these divergent findings is unclear. We suggest that, because of the relative inability of GPC-mediated fusion pores to enlarge, the small fluorescent dye mixing-based fusion assay employed in our study more sensitively detects cell fusion than the syncytium- or reporter protein-based assays used by others.

We also characterized the nature of a fusion block imposed by ST-193, a pan-arenavirus fusion inhibitor that targets the interface between GP2 and the stable signal peptide of the GPC [62]. At a ST-193 concentration that almost completely inhibits LASV GPC-mediated cell fusion, the compound still permits fusion to proceed to a hemifusion stage. However, for the most part, these are not on-path hemifusion structures that naturally resolve into full fusion upon removing the inhibitor; their existence can only be revealed by CPZ treatment that destabilizes the hemifusion diaphragm. These results demonstrate that, under our experimental conditions, ST-193 does not block early pH-induced conformational changes in GPC. The tendency to form dead-end hemifusion structures may suggest a role for the stable signal peptide in late stages of fusion. Alternatively, non-productive fusion pathways can be favored by a less efficient GPC activation in the presence of ST-193.

Another striking feature of Old and New World arenaviruses, which use distinct cellular receptors for infection [1–3,83], is that, in contrast to the overwhelming majority of enveloped viruses, arenavirus entry/fusion is resistant to restriction by IFITMs [35,78,79]. We have recently shown that IFITM3 exerts broad antiviral activity by blocking fusion at a hemifusion stage through modulating the properties of the cytoplasmic leaflet of endosomal membranes [84]. One might think that these findings suggest that the GPC fusion machinery is more robust than other viral glycoproteins and is therefore able to overcome IFITM-mediated restriction. However, we have shown that: (1) as is the case for other viral proteins, GPC cannot overcome the increased membrane bending energy imposed by lyso-PC incorporation (Fig 4B); and (2) LASV appears to avoid IFITM3 restriction by entering and fusing with endosomes devoid of this antiviral protein [78]. It thus appears that New and Old World arenavirus trafficking pathways converge to unique cellular compartments devoid of IFITMs.

The key finding of this study is the discovery that LASV GPC-mediated cell-cell and pseudovirus-cell fusion are enhanced by the late endosome-resident lipid, BMP (Figs 5–7). Since GPC-mediated fusion is not modulated by another anionic lipid, DOPS, the effect of BMP appears specific. Importantly, BMP modulates the late stages of LASV GPC-mediated cell fusion by promoting both the transition from hemifusion to full fusion and the growth of fusion pores (Figs 5D, 5E and 6). BMP is an unusual lipid that is highly concentrated in late endosomes/lysosomes; it is involved in intracellular cholesterol transport and, through binding to Alix, in biogenesis of multivesicular bodies [65,66,73,85,86]. Its intrinsic curvature is modulated by pH and calcium ions, as evidenced by the pH gradient-driven inward budding and low pH-dependent liposome fusion observed in BMP-containing liposomes [63,85].

In contrast to cell-cell fusion, there was no detectable enhancement of viral entry through the endocytic pathway upon exogenous addition of this lipid (S5 Fig). We surmise that exogenous addition of BMP fails to augment LASV pseudovirus fusion because late endosomes contain optimal amounts of BMP. It is also possible that exogenous BMP is trafficked to distinct compartments that are not used by LASV for entry. We were able, however, to demonstrate BMP-dependence of LASVpp fusion using the NPC1 mutant expressing CHO cells that accumulate cholesterol and BMP in late endosomes.

The role of lipids in promoting viral fusion has been reported for alphaviruses (e.g., [87,88]), flaviviruses (e.g., [89,90]), orthomyxoviruses [91], rhabdoviruses [69] and lentiviruses [48]). It should be stressed that, unlike the fusion of Dengue virus that is non-specifically promoted by anionic lipids [89], LASV fusion is specifically enhanced by BMP. We have also observed a similar effect of BMP on fusion of VSV-G protein pseudotyped particles with supported lipid bilayers [92].

How does BMP specifically promote LASV fusion with late endosomes? Since this lipid appears to be present in both inner and cytoplasmic leaflets of endosomal membranes [68], it is feasible that BMP interacts directly with LASV GPC and augments functional oligomerization and/or refolding of this protein into the final 6-helix bundle structure. It is currently unclear whether BMP in the cytoplasmic leaflet may destabilize a hemifusion diaphragm and thereby promote the transition to full fusion. This possibility appears less likely, because one would expect to see a non-specific enhancement of fusion mediated by other viral glycoproteins, which is not observed in our experiments. The role of BMP in dilation of GPC-mediated fusion pores may explain its equally notable effect on fusion upon pretreatment of either effector or target cells (S2B Fig). It is expected that this lipid incorporates into the fusion pore through either GPC-expressing or target cell membrane.

Together, our findings suggest the following model for LASV entry into cells. LASV fusion may be initiated in early LAMP1-containing endosomes, but here it can only culminate in the formation of a stable hemifusion intermediate. This intermediate resolves into full fusion after virus enters late endosomes enriched in BMP.

Materials and methods

Cells and reagents

COS7 cells and HEK293T cells were maintained in Eagle's Medium with glucose, L-glutamine, and sodium pyruvate, supplemented with 10% Cosmic Calf Serum (HyClone, Logan, Utah), penicillin/streptomycin (ThermoFisher, Waltham, MA Cat# 15140–122). The quail QT6 and chicken DF-1 cells were obtained from ATCC (Manassas, VA). QT6 cultured in F-12K medium with 2 mM L-glutamine, 10% tryptose phosphate broth and 5% calf serum. DF-1 cells were grown in DMEM with 4.5 g/l glucose, L-glutamine, sodium pyruvate and 10% fetal bovine serum. Parental CHO and CHO-NPC1mut cells (clone 10–3, [75]) provided by Joseph Goldstein (UT Southwestern) were grown in alpha-MEM (Quality Biological, Gaithersburg, MD) medium complemented with 10% inactivated fetal bovine serum (FBS, Atlanta Biologicals, Flowery Branch, GA), and 100 units/mL of penicillin-streptomycin (Gemini Bio-Products, Sacramento, CA, USA).

COS7 cells grown to ~60% confluency on a 35 mm culture dish were transfected with 4 μg of the plasmid expressing the Lassa virus GPC (Josiah strain, a kind gift from F.-L. Cosset [34] using a standard calcium phosphate method. Where indicated, HEK293T and QT6 cells were transfected with the plasmids expressing the wild-type LAMP1 or the LAMP1 D384 mutant (a gift from Ron Riskin (Weizmann Institute, Israel) (32), using a calcium phosphate method. LAMP1-mRFP plasmid was from Addgene (Cat# 1817).

The HIV-1-based packaging vector pR9ΔEnv was from Dr. Chris Aiken (Vanderbilt University). The pMM310 vector expressing BlaM-Vpr, psPAX2 lentiviral packaging vector, pcRev vector, pMDG-VSVG plasmid expressing VSV-G, H1N1 WSN HA and NA, phCMV-Lassa GPC or pcDNA3.1-Ebola GP (Zaire) expression vectors were described previously [35,93]. The pNL4-3.Luc.R-E- packaging vector was obtained through the NIH AIDS Reagent Program (from Dr. Nathaniel Landau [94]).

Lipids: DOPC (1,2-dioleoyl-sn-glycero-3-phosphocholine), DOPS (1,2-dioleoyl-sn-glycero-3-phospho-L-serine), BMP (bis(monooleoylglycero)phosphate (S,R Isomer)) and lyso-PC (lauroyl-lysoPC) were obtained from Avanti Polar Lipids (Alabaster, AL). Chlorpromazine was purchased from Sigma (Cat# C8138, St. Louis, MO). A soluble fragment of human LAMP1 was obtained from Origene Protein (Cat# TP720784). The LASV fusion inhibitor ST-193 was from Medchem Express (NJ, Cat.# HY-101441). Annexin V labeled with AF647 was obtained from Invitrogen (ThermoFisher, Cat# A232004). Mouse monoclonal anti-BMP antibody 6C4, neuraminidase and TPCK-treated trypsin were purchased from Millipore Sigma (Burlington, MA, Cat# MABT837, N2876 and T4376). FITC-conjugated anti-human LAMP1 antibody CD107a (Cat# A14750) and mouse IgG1κ isotype control antibody (Cat# 14-4714-85) were purchased from ThermoFisher. Fatty acid-free BSA was from Sigma (Cat# A1933).

Pseudovirus production and single-cycle infection assay

The single-cycle infection-competent pseudotyped viruses were generated by transfecting HEK293T/17 cells grown to ~75% confluency in 10-cm dishes with JetPRIME transfection reagent (Polyplus-transfection, Illkirch-Graffenstaden, France). The cells and plasmid transfection mix were incubated for 14 h at 37˚C, 5% CO_2, followed by incubation with fresh medium for another ~34 h. The viral supernatants were filtered through 0.45 μm polyethersulfone filters (PES, VWR), aliquoted and stored at -80˚C. The p24 content of pseudovirus preparations was quantified by ELISA, as described previously [95]. To generate luciferase-encoding pseudoviruses, HEK293T/17 cells were transfected with 6 μg pNL4-3.Luc.R-E-, 0.5 μg pcRev and 4 μg Lassa-GPC or 2.5 μg each of WSN HA- and NA-expressing plasmids, respectively. For the BlaM assay, HEK293T/17 cells were transfected with 4 μg pR9ΔEnv, 2 μg BlaM-Vpr, pcRev and Lassa-GPC (4 μg), WSN HA/NA (5 μg) or VSV-G (1.5 μg), or Ebola-GP (1 μg). To produce shRNA encoding pseudoviruses, HEK293T/17 cells were transfected with 1.5 μg pMDG-VSVG, 3 μg psPAX2, and 4 μg pooled shRNA plasmids.

For the infectivity assay, target cells (~2×10^4 cells/well in black-clear bottom 96-well plates) and virus (0.2 ng p24/well) were centrifuged at 1550×*g* for 30 min at 4˚C. Unbound virus was washed off, 75 μL/well of growth medium was added, and cultured at 37˚C, 5% CO_2. Forty-eight hours post-infection, the samples were incubated for 5 min at room temperature with equivalent volumes of Bright-Glo™ firefly luciferase substrate (Promega, Madison, WI), and the luciferase signal was measured using a TopCount NXT plate reader (PerkinElmer Life Sciences, Waltham, MA, USA).

shRNA knock down and Western blotting

For shRNA knock down, 5 validated LAMP1 shRNAs were ordered from human Mission lentiviral library (Sigma). HEK293T/17 and A549 cells grown to ~70% confluency in 6-well plates were transduced with 0.5 ng p24/well of shRNA pseudoviruses, with centrifugation at 1550×*g* for 30 min at 4˚C. Unbound viruses were removed, fresh medium was added, and samples were incubated at 37˚C, 5% CO_2. Twenty-four hours post-transduction, cells were transferred to 10-cm dishes in the presence of 1.5 μg puromycin. After 4 days of selection, cells were processed for Western blotting, as described in [78]. The LAMP1 protein was detected with rabbit anti-LAMP1 (Sigma, Cat# SAB3500285) and horseradish peroxidase-conjugated mouse anti-rabbit (Millipore, Cat# AP188P), using ECL Prime chemiluminescence reagent (GE Healthcare). The chemiluminescence signal was detected using a XR^+ gel doc (Bio-Rad). Densitometry analysis was done using Image Lab software (Bio-Rad).

Cell-cell fusion assay

Effector and target cells were labeled and cell-cell fusion quantified, as described in [46]. Briefly, ~2x10^6 COS7 and target (HEK293T or avian cells, as indicated) cells were loaded with 1.5 μM calcein-AM or 20 μM CMAC (Invitrogen), respectively, for 30 min at 37˚C. Labeled effector COS7 cells and target HEK293T or QT6 cells were detached from culture dishes using a non-enzymatic solution (divalent-free PBS/EGTA/EDTA). Effector and target cells were resuspended in PBS^{++} or PBS^{++} supplemented with 1 mg/ml BSA, as indicated, mixed at an 1:1 ratio in a test tube and added to wells of an 8-well slide (Thermo Fisher) coated with poly-lysine (Sigma, Cat# P1274). Cells were allowed to adhere and establish contacts for 30 min at room temperature. The density of cells was adjusted to minimize aggregation and, at the same time, ensure sufficient cell-cell contacts to allow subsequent fusion. Next, the pH was lowered for 10–20 min at room temperature or at 37˚C to the indicated value, using a citric acid-sodium citrate buffer. Following the acid trigger step, cells were returned to pH 7.2 PBS^{++} and further incubated at 37˚C for 30–60 min. Cell-cell fusion was detected by fluorescence microscopy based upon the appearance of calcein- and CMAC-positive cells, as described previously [46]. The extent of fusion was determined by normalizing the number of double-positive cells per field to the total number of effector/target cell contacts. Typically, 10 randomly selected image fields, each containing ~10 effector/target cell pairs, were analyzed for each well.

Arresting fusion intermediates and testing the effects of exogenous lipids

To reveal the presence of unresolved hemifusion structures after triggering fusion of effector and target cells by exposure to low pH, cells were treated with 0.5 mM CPZ in PBS^{++} for 1 min at room temperature. To capture cells at a cold-arrested stage (CAS), effector/target cell pairs were chilled on ice and exposed to pH 5.0 at 4˚C for 10 min. Cells were returned to PBS^{++} and either incubated at 37˚C to allow fusion or treated with 0.5 mM CPZ for 1 min and immediately counted under the microscope.

To capture cell-cell fusion at a lipid-arrested stage (LAS), effector/target cell pairs were pre-treated with 285μM stearoyl lyso-PC in PBS for 30 min at room temperature followed by exposure to a pH 5.0 buffer for 10 min at room temperature in the presence of lyso-PC. Cells were returned to neutral pH and either incubated at 37˚C in the presence of lyso-PC or washed with delipidated BSA (2 mg/ml, Sigma) to remove lyso-PC and then maintained at 37˚C for 30 min.

To assess the effect of lipids on cell fusion, COS7 cells mixed with target QT6 or HEK293T cells were allowed to adhere to a poly-lysine coated slide for 30 min at room temperature. Lipids DOPC, DOPS or BMP were diluted from 5 mg/ml stock solutions in ethanol to a final concentration of 10 or 40 μg/ml in PBS^{++} supplemented with 1 mg/ml BSA (Sigma) and immediately added to cells. Cells were incubated with lipids for 20 min at room temperature and exposed to acidic buffers at the pH and temperature indicated. Cell-cell fusion was scored after returning the cells to neutral pH and incubating for additional 30 min at 37˚C. The effects of exogenous lipids on the late steps of LASV fusion were assessed by capturing the fusion reaction at CAS (exposure to a cold pH 5.0 buffer for 10 min) and adding 10 μg/ml of indicated lipids at neutral pH and incubating for 10 min at room temperature. Cells were then shifted to 37˚C and incubated 30 min to allow fusion to occur.

Pore permeability measurements

Permeability of pores between effector and target cells was measured, as previously described [70,71]. Briefly, GPC-transfected COS7 cells were loaded with calcein-AM dye, premixed with target HEK293T cells, and allowed to adhere to poly-lysine coated coverslips for 30 min at room temperature. Pieces of coverslip with cells were transferred into a home-made imaging

chamber with an IR-absorbing coverslip at the bottom; the chamber contained a pH 5.0 buffer. Temperature was quickly and locally raised and maintained at 37˚C by illuminating the absorbing coverslip with an IR diode [70,71]. Dye transfer was monitored with a Fluoview300 laser scanning confocal microscope (Olympus IX70, America, Melville, NY) using an UPlanApo 60X/1.20NA water-immersion objective. Total fluorescence intensities of effector and target cells over time were determined using two manually drawn ROIs, and the relative pore permeability was calculated using the equation: $P(t) = Q(t)\cdot(dI_t/dt)/(I_e(t)—I_t(t)) = -Q(t)\cdot(dI_e/dt)(I_e(t)—I_t(t))$, where I_t and I_e are fluorescence intensities of target and effector cell, respectively, and Q(t) is a correction factor to account for the temperature-dependence of the diffusion coefficient of calcein [70]. To assess the effect of exogenous lipids, pieces of a coverslip with effector and target cells were pretreated with BMP or DOPC (20 μg/ml), as described above, for 10 min at room temperature, prior to transferring the coverslips to the imaging chamber containing a pH 5.0 buffer; temperature-jump experiments were then performed.

Virus-cell fusion assay

Target cells were seeded in 96-well black-clear bottom plates one day before the experiment to reach ~90% confluency the next morning. Cells were pretreated with 0.2 μM Bafilomycin A1 (Santa Cruz Biotech., Cat# SC201550) for 1 h at 37˚C. Cells were then spinoculated with various amounts of LASV, JUNV or IAV pseudoviruses containing BlaM-Vpr in HBSS supplemented with 10% FBS at 3,000 rpm for 30 min at room temperature. Cells were washed to remove unbound viruses, treated with 40 μg/ml of indicated lipids dissolved in PBS^{++} supplemented with 1 mg/ml BSA for 10 min at room temperature and exposed to a pH 5.0 buffer for 30 min at 37˚C. Cells were loaded with the BlaM CCF-4-AM substrate (Thermo Fisher Scientific) and incubated overnight at 16˚C. For the regular virus-cell fusion assay, cells were pretreated with lipids as described above, spinoculated with pseudoviruses and placed into a CO_2 incubator for 2 h at 37˚C. The resulting cytosolic BlaM activity was measured on a Wallac 1420 Victor2 (PerkinElmer, Turku, Finland) fluorescence microplate reader at 460nm (blue) and 528nm (green), using 400nm excitation.

For virus-cell fusion experiments involving antibodies, the target cells grown to ~60% confluency in black-clear bottom 96-well plates were starved for 6 h and incubated for 15 h with 50 μg/mL antibodies in growth medium. For experiments with CHO and CHO.NPC1 mutant cells, cells were grown to ~95% confluency in black-clear bottom 96-well plates. Pseudoviruses containing BlaM-Vpr were bound to cells, as described above, and incubated for 2 h at 37˚C, 5% CO_2. Cells were then loaded with CCF-4-AM substrate, and incubated overnight at 11˚C. The BlaM activity was measured using SpectraMax i3X (Molecular Devices, Sunnyvale, CA) or Synergy-H1 (BioTeck, Winooski, VT) fluorescence plate reader.

Immunofluorescence and cholesterol staining

COS7 cells were treated for 20 min at room temperature with the indicated lipids that were dissolved at 10 μg/ml in PBS supplemented with 1mg/ml BSA. Cells then washed and fixed with 4% PFA (Electron Microscopy Sciences, Cat# 15710). The presence of DOPS on the cell surface was detected using Annexin V labeled with AlexaFluor647 (1:200 dilution of the stock). Exogenous BMP on the cell surface was detected using the mouse anti-BMP 6C4 monoclonal antibody followed by incubation with goat anti-mouse IgG conjugated with AlexaFluor488 (Invitrogen).

To determine the levels and patterns of BMP and cholesterol expression, cells were washed with PBS^{++}, fixed with 4% PFA and permeabilized with 125 μg/ml digitonin and incubated with mouse anti-BMP 6C4 antibody (1:200, Millipore Sigma). Cells were washed and

incubated with AF488-conjugated goat anti-mouse IgG (1:500, ThermoFisher) and 0.25 mg/ml filipin (Sigma). Cell nuclei were stained with far-red NucSpot dye (1:1000, Biotinium). Images were acquired on a Zeiss LSM 880 microscope using a plan-apochromat 63X/1.4NA oil objective. BMP and cholesterol levels were determined by the integrating fluorescence intensity per cell after background subtraction.

To assess the cell surface levels of LAMP1, QT6 cells were transfected with LAMP1, or LAMP1mut plasmids or mock- transfected. After 48 h, ~10^6 cells were detached using a non-enzymatic solution and incubated with the FITC-conjugated anti-LAMP1 antibody CD107a (ThermoFisher, A14750) diluted 1:100 in PBS/0.1% Na-azide/5% Calf Serum for 1 h at room temperature in the dark. Cells were washed, resuspended in 800 μL of divalent-free PBS, and analyzed on a Guava EasyCyte system (Guava Technologies, Inc. Hayward CA USA).

Supporting information

S1 Fig. Surface expression of human LAMP1 in transfected QT6 cells measured by flow cytometry. QT6 cells were mock transfected or transfected with human LAMP1 or LAMP1 mutant. Cell surface expression was measured by flow cytometry after staining with FITC-conjugated anti-LAMP1 antibody. (A) Histograms of LAMP1 signals from untransfected QT6 cells and cells expressing wild-type or mutant human LAMP1 from a representative experiment. (B) Average MFI values for cells in panel (A) from three independent experiments. Error bars are SEM.
(TIF)

S2 Fig. LASV GPC inhibition by ST-193 and inactivation at low pH. (A) Dose-dependent inhibition of LASV GPC-mediated cell-cell fusion by the arenavirus fusion inhibitor ST-193. LASV GPC-expressing COS7 cells (loaded with calcein-AM) and HEK293T cells transfected with LAMP1mut (loaded with CMAC) were mixed at a 1:1 ratio, adhered to poly-lysine coated coverslips and incubated for 30 min at room temperature. Cell fusion was triggered by exposure to pH 6.2 for 10 min at room temperature (suboptimal trigger) in the presence or absence of the indicated concentration of ST-193. The results are means and SEM from three independent experiments. (B) GPC-expressing COS7 cells were pretreated with a pH 4.0 buffer for 10 min at 37˚C followed by co-incubation with target HEK293T cells for 10 min at neutral pH, room temperature, to establish cell-cell contacts. Effector-target cell complexes were then exposed to pH 6.2 for 10 min at room temperature and further incubated at neutral pH for 1 h at 37˚C. The results are means and SEM from three independent experiments.
(TIF)

S3 Fig. Anti-BMP antibody inhibits LASVpp fusion with A549 cells. Human A549 cells were starved for 6 h and incubated with 50 μg/ml of anti-BMP or control IgG1κ antibodies for 15 h to allow antibody internalization by fluid-phase uptake before infecting with LASVpp or IAVpp. Virus-cell fusion was measured using a BlaM assay. Control samples were treated with 70 mM NH_4Cl to block endosomal entry of viruses. The results are means and SD from 2 independent experiments performed in duplicates.
(TIF)

S4 Fig. Incorporation of exogenously added lipids into cells and their effects on GPC-mediated cell-cell fusion. (A) *Top*: Representative images of Annexin V-stained COS7 cells. Cells were pretreated with 10 μg/ml DOPC (negative control) or DOPS in BSA for 20 min at room temperature, washed and stained with 5 μg/ml of AlexaFluor647-labeled Annexin V (ThermoFisher) for 1 h at 4˚C. *Bottom*: Cells were pretreated with 10 μg/ml BMP in BSA or mock treated, washed, fixed with 4% PFA and incubated with anti-BMP antibody (1:250

dilution) for 1h at 4˚C, followed by incubation with goat anti mouse AlexaFluor488-conjugated second antibody (1:1000 dilution). Images were acquired on a Fluoview300 microscope (Olympus, Melville, NY), using an UPlanApo 60X/1.20NA water-immersion objective and standard eGFP and Cy5 filter cubes for Annexin V and BMP immunostaining, respectively. (B) Effect of BMP on cell fusion upon incorporation into target or effector cells. GPC-expressing COS7 cells or target HEK293T cells were pretreated in suspension with either DOPC or BMP at 10 μg/ml for 20 min at room temperature. Cells were washed mixed with target or effector cells, respectively, and allowed to adhere to glass slides for 15 min at room temperature. Fusion was triggered by exposure to pH 5.0 for 20 min, 37˚C. The results are plotted as fold-increase in cell-cell fusion by BMP relative to DOPC. Data are means and SEM from four independent experiments.
(TIF)

S5 Fig. Effect of exogenous lipids on LASV pseudovirus fusion. (A, B) Two independent experiments showing the effect of exogenously added DOPC, DOPS and BMP (40 μg/ml in BSA-containing PBS) on LASVpp fusion with HEK293T cells. The LASVpp fusion under these conditions was measured by a BlaM assay using the blue/green ratio of fluorescence of a BlaM substrate that was loaded into cells. (C, D) Same as in panel A, but showing the result of two experiments of LASVpp fusion with avian DF-1 cells. No significant changes in the BlaM signal were observed after cell pretreatment with any of the lipids. (E) Lipid-dependence of forced pseudovirus fusion with the plasma membrane. HEK293T cells were pretreated with 0.2 μM BafA1 for 1h at 37˚C, washed and spinoculated with LASVpp or IAVpp for 30 min at room temperature. Unbound virus was removed, and cells were treated with 40 μg/ml of the indicated lipids dissolved in BSA for 10 min at room temperature. Virus fusion was then induced by exposure to pH 5.0 for 30 min at 37˚C in the presence of lipids. The cells were next loaded with the BlaM substrate, and the extent of virus-cell fusion was measured by a BlaM assay after overnight incubation, as described in Materials and Methods. The results are means and SEM from 3 independent experiments (LASVpp) and two independent experiments (IAVpp).
(TIF)

Acknowledgments

The authors wish to thank F.-L. Cosset (University Claude Bernard Lyon) for the gift of the LASV GPC plasmid, Jack Nunberg (University of Montana) for the plasmid encoding wild-type and mutant GPC of Junin virus, Joseph Goldstein (UT Southwestern) for CHO and CHO.NPC1mut cells, and Ron Riskin (Weizmann Institute) for LAMP1 and LAMP1mut expressing vectors. We thank Xiangyang Guo for help with experiments involving lipid delivery into cells, Gokul Raghunath and other members of the Melikyan laboratory for critical reading of the manuscript and constructive suggestions.

Author Contributions

Conceptualization: Fredric S. Cohen, Gregory B. Melikyan.

Formal analysis: Ruben M. Markosyan, Mariana Marin, You Zhang, Gregory B. Melikyan.

Investigation: Ruben M. Markosyan, Mariana Marin, You Zhang.

Methodology: Ruben M. Markosyan, Mariana Marin, You Zhang.

Resources: Gregory B. Melikyan.

Supervision: Fredric S. Cohen, Gregory B. Melikyan.

Writing – original draft: Gregory B. Melikyan.

Writing – review & editing: Ruben M. Markosyan, Mariana Marin, You Zhang, Fredric S. Cohen, Gregory B. Melikyan.

References

1. Fedeli C, Moreno H, Kunz S. Novel Insights into Cell Entry of Emerging Human Pathogenic Arenaviruses. J Mol Biol. 2018; 430(13):1839–52. https://doi.org/10.1016/j.jmb.2018.04.026 PMID: 29705070
2. Nunberg JH, York J. The curious case of arenavirus entry, and its inhibition. Viruses. 2012; 4(1):83–101. https://doi.org/10.3390/v4010083 PMID: 22355453
3. Rojek JM, Kunz S. Cell entry by human pathogenic arenaviruses. Cell Microbiol. 2008; 10(4):828–35. https://doi.org/10.1111/j.1462-5822.2007.01113.x PMID: 18182084
4. Martinez MG, Cordo SM, Candurra NA. Characterization of Junin arenavirus cell entry. The Journal of general virology. 2007; 88(Pt 6):1776–84. https://doi.org/10.1099/vir.0.82808-0 PMID: 17485539
5. Rojek JM, Sanchez AB, Nguyen NT, de la Torre JC, Kunz S. Different mechanisms of cell entry by human-pathogenic Old World and New World arenaviruses. J Virol. 2008; 82(15):7677–87. https://doi.org/10.1128/JVI.00560-08 PMID: 18508885
6. Pasqual G, Rojek JM, Masin M, Chatton JY, Kunz S. Old world arenaviruses enter the host cell via the multivesicular body and depend on the endosomal sorting complex required for transport. PLoS Pathog. 2011; 7(9):e1002232. https://doi.org/10.1371/journal.ppat.1002232 PMID: 21931550
7. Rojek JM, Perez M, Kunz S. Cellular entry of lymphocytic choriomeningitis virus. J Virol. 2008; 82(3):1505–17. https://doi.org/10.1128/JVI.01331-07 PMID: 18045945
8. Oppliger J, Torriani G, Herrador A, Kunz S. Lassa Virus Cell Entry via Dystroglycan Involves an Unusual Pathway of Macropinocytosis. J Virol. 2016; 90(14):6412–29. https://doi.org/10.1128/JVI.00257-16 PMID: 27147735
9. Iwasaki M, Ngo N, de la Torre JC. Sodium hydrogen exchangers contribute to arenavirus cell entry. J Virol. 2014; 88(1):643–54. https://doi.org/10.1128/JVI.02110-13 PMID: 24173224
10. York J, Nunberg JH. Role of the stable signal peptide of Junin arenavirus envelope glycoprotein in pH-dependent membrane fusion. J Virol. 2006; 80(15):7775–80. https://doi.org/10.1128/JVI.00642-06 PMID: 16840359
11. Quirin K, Eschli B, Scheu I, Poort L, Kartenbeck J, Helenius A. Lymphocytic choriomeningitis virus uses a novel endocytic pathway for infectious entry via late endosomes. Virology. 2008; 378(1):21–33. https://doi.org/10.1016/j.virol.2008.04.046 PMID: 18554681
12. Burri DJ, da Palma JR, Kunz S, Pasquato A. Envelope glycoprotein of arenaviruses. Viruses. 2012; 4(10):2162–81. https://doi.org/10.3390/v4102162 PMID: 23202458
13. Hastie KM, Igonet S, Sullivan BM, Legrand P, Zandonatti MA, Robinson JE, et al. Crystal structure of the prefusion surface glycoprotein of the prototypic arenavirus LCMV. Nat Struct Mol Biol. 2016; 23(6):513–21. https://doi.org/10.1038/nsmb.3210 PMID: 27111888
14. Hastie KM, Zandonatti MA, Kleinfelter LM, Heinrich ML, Rowland MM, Chandran K, et al. Structural basis for antibody-mediated neutralization of Lassa virus. Science. 2017; 356(6341):923–8. https://doi.org/10.1126/science.aam7260 PMID: 28572385
15. Igonet S, Vaney MC, Vonrhein C, Bricogne G, Stura EA, Hengartner H, et al. X-ray structure of the arenavirus glycoprotein GP2 in its postfusion hairpin conformation. Proceedings of the National Academy of Sciences of the United States of America. 2011; 108(50):19967–72. https://doi.org/10.1073/pnas.1108910108 PMID: 22123988
16. Crispin M, Zeltina A, Zitzmann N, Bowden TA. Native functionality and therapeutic targeting of arenaviral glycoproteins. Current opinion in virology. 2016; 18:70–5. https://doi.org/10.1016/j.coviro.2016.04.001 PMID: 27104809
17. Shulman A, Katz M, Cohen-Dvashi H, Greenblatt HM, Levy Y, Diskin R. Variations in Core Packing of GP2 from Old World Mammarenaviruses in their Post-Fusion Conformations Affect Membrane-Fusion Efficiencies. J Mol Biol. 2019; 431(11):2095–111. https://doi.org/10.1016/j.jmb.2019.04.012 PMID: 31004664
18. Messina EL, York J, Nunberg JH. Dissection of the role of the stable signal peptide of the arenavirus envelope glycoprotein in membrane fusion. J Virol. 2012; 86(11):6138–45. https://doi.org/10.1128/JVI.07241-11 PMID: 22438561

19. Agnihothram SS, York J, Nunberg JH. Role of the stable signal peptide and cytoplasmic domain of G2 in regulating intracellular transport of the Junin virus envelope glycoprotein complex. J Virol. 2006; 80 (11):5189–98. https://doi.org/10.1128/JVI.00208-06 PMID: 16698999

20. York J, Romanowski V, Lu M, Nunberg JH. The signal peptide of the Junin arenavirus envelope glycoprotein is myristoylated and forms an essential subunit of the mature G1-G2 complex. J Virol. 2004; 78 (19):10783–92. https://doi.org/10.1128/JVI.78.19.10783-10792.2004 PMID: 15367645

21. Bederka LH, Bonhomme CJ, Ling EL, Buchmeier MJ. Arenavirus stable signal peptide is the keystone subunit for glycoprotein complex organization. mBio. 2014; 5(6):e02063. https://doi.org/10.1128/mBio.02063-14 PMID: 25352624

22. York J, Nunberg JH. Myristoylation of the Arenavirus Envelope Glycoprotein Stable Signal Peptide Is Critical for Membrane Fusion but Dispensable for Virion Morphogenesis. J Virol. 2016; 90(18):8341–50. https://doi.org/10.1128/JVI.01124-16 PMID: 27412594

23. Saunders AA, Ting JP, Meisner J, Neuman BW, Perez M, de la Torre JC, et al. Mapping the landscape of the lymphocytic choriomeningitis virus stable signal peptide reveals novel functional domains. J Virol. 2007; 81(11):5649–57. https://doi.org/10.1128/JVI.02759-06 PMID: 17376927

24. Cao W, Henry MD, Borrow P, Yamada H, Elder JH, Ravkov EV, et al. Identification of alpha-dystroglycan as a receptor for lymphocytic choriomeningitis virus and Lassa fever virus. Science. 1998; 282 (5396):2079–81. https://doi.org/10.1126/science.282.5396.2079 PMID: 9851928

25. Jae LT, Raaben M, Herbert AS, Kuehne AI, Wirchnianski AS, Soh TK, et al. Virus entry. Lassa virus entry requires a trigger-induced receptor switch. Science. 2014; 344(6191):1506–10. https://doi.org/10.1126/science.1252480 PMID: 24970085

26. Li S, Sun Z, Pryce R, Parsy ML, Fehling SK, Schlie K, et al. Acidic pH-Induced Conformations and LAMP1 Binding of the Lassa Virus Glycoprotein Spike. PLoS Pathog. 2016; 12(2):e1005418. https://doi.org/10.1371/journal.ppat.1005418 PMID: 26849049

27. Raaben M, Jae LT, Herbert AS, Kuehne AI, Stubbs SH, Chou YY, et al. NRP2 and CD63 Are Host Factors for Lujo Virus Cell Entry. Cell host & microbe. 2017; 22(5):688–96 e5. https://doi.org/10.1016/j.chom.2017.10.002 PMID: 29120745

28. Lavanya M, Cuevas CD, Thomas M, Cherry S, Ross SR. siRNA screen for genes that affect Junin virus entry uncovers voltage-gated calcium channels as a therapeutic target. Science translational medicine. 2013; 5(204):204ra131. https://doi.org/10.1126/scitranslmed.3006827 PMID: 24068738

29. Radoshitzky SR, Abraham J, Spiropoulou CF, Kuhn JH, Nguyen D, Li W, et al. Transferrin receptor 1 is a cellular receptor for New World haemorrhagic fever arenaviruses. Nature. 2007; 446(7131):92–6. https://doi.org/10.1038/nature05539 PMID: 17287727

30. Flanagan ML, Oldenburg J, Reignier T, Holt N, Hamilton GA, Martin VK, et al. New world clade B arenaviruses can use transferrin receptor 1 (TfR1)-dependent and -independent entry pathways, and glycoproteins from human pathogenic strains are associated with the use of TfR1. J Virol. 2008; 82(2):938–48. https://doi.org/10.1128/JVI.01397-07 PMID: 18003730

31. Hulseberg CE, Feneant L, Szymanska KM, White JM. Lamp1 Increases the Efficiency of Lassa Virus Infection by Promoting Fusion in Less Acidic Endosomal Compartments. mBio. 2018; 9(1). https://doi.org/10.1128/mBio.01818-17 PMID: 29295909

32. Cohen-Dvashi H, Israeli H, Shani O, Katz A, Diskin R. Role of LAMP1 Binding and pH Sensing by the Spike Complex of Lassa Virus. J Virol. 2016; 90(22):10329–38. https://doi.org/10.1128/JVI.01624-16 PMID: 27605678

33. Bulow U, Govindan R, Munro JB. Acidic pH Triggers Lipid Mixing Mediated by Lassa Virus GP. Viruses. 2020; 12(7). https://doi.org/10.3390/v12070716 PMID: 32630688

34. Cosset FL, Marianneau P, Verney G, Gallais F, Tordo N, Pecheur EI, et al. Characterization of Lassa virus cell entry and neutralization with Lassa virus pseudoparticles. J Virol. 2009; 83(7):3228–37. https://doi.org/10.1128/JVI.01711-08 PMID: 19153226

35. Desai TM, Marin M, Chin CR, Savidis G, Brass AL, Melikyan GB. IFITM3 restricts influenza A virus entry by blocking the formation of fusion pores following virus-endosome hemifusion. PLoS Pathog. 2014; 10(4):e1004048. https://doi.org/10.1371/journal.ppat.1004048 PMID: 24699674

36. Melikyan GB, Barnard RJ, Abrahamyan LG, Mothes W, Young JA. Imaging individual retroviral fusion events: from hemifusion to pore formation and growth. Proceedings of the National Academy of Sciences of the United States of America. 2005; 102(24):8728–33. https://doi.org/10.1073/pnas.0501864102 PMID: 15937118

37. Melikyan GB, White JM, Cohen FS. GPI-anchored influenza hemagglutinin induces hemifusion to both red blood cell and planar bilayer membranes. The Journal of cell biology. 1995; 131(3):679–91. https://doi.org/10.1083/jcb.131.3.679 PMID: 7593189

38. Chernomordik LV, Leikina E, Kozlov MM, Frolov VA, Zimmerberg J. Structural intermediates in influenza haemagglutinin-mediated fusion. Mol Membr Biol. 1999; 16(1):33–42. https://doi.org/10.1080/096876899294733 PMID: 10332735

39. Zaitseva E, Mittal A, Griffin DE, Chernomordik LV. Class II fusion protein of alphaviruses drives membrane fusion through the same pathway as class I proteins. The Journal of cell biology. 2005; 169 (1):167–77. https://doi.org/10.1083/jcb.200412059 PMID: 15809312

40. Kemble GW, Danieli T, White JM. Lipid-anchored influenza hemagglutinin promotes hemifusion, not complete fusion. Cell. 1994; 76(2):383–91. https://doi.org/10.1016/0092-8674(94)90344-1 PMID: 8293471

41. Abrahamyan LG, Markosyan RM, Moore JP, Cohen FS, Melikyan GB. Human immunodeficiency virus type 1 Env with an intersubunit disulfide bond engages coreceptors but requires bond reduction after engagement to induce fusion. J Virol. 2003; 77(10):5829–36. https://doi.org/10.1128/jvi.77.10.5829-5836.2003 PMID: 12719576

42. Harmon B, Campbell N, Ratner L. Role of Abl kinase and the Wave2 signaling complex in HIV-1 entry at a post-hemifusion step. PLoS Pathog. 2010; 6(6):e1000956. https://doi.org/10.1371/journal.ppat.1000956 PMID: 20585556

43. Markosyan RM, Miao C, Zheng YM, Melikyan GB, Liu SL, Cohen FS. Induction of Cell-Cell Fusion by Ebola Virus Glycoprotein: Low pH Is Not a Trigger. PLoS Pathog. 2016; 12(1):e1005373. https://doi.org/10.1371/journal.ppat.1005373 PMID: 26730950

44. Melikyan GB, Barnard RJ, Markosyan RM, Young JA, Cohen FS. Low pH Is Required for Avian Sarcoma and Leukosis Virus Env-Induced Hemifusion and Fusion Pore Formation but Not for Pore Growth. J Virol. 2004; 78(7):3753–62. https://doi.org/10.1128/jvi.78.7.3753-3762.2004 PMID: 15016895

45. Melikyan GB, Markosyan RM, Brener SA, Rozenberg Y, Cohen FS. Role of the cytoplasmic tail of ecotropic moloney murine leukemia virus Env protein in fusion pore formation. J Virol. 2000; 74(1):447–55. https://doi.org/10.1128/jvi.74.1.447-455.2000 PMID: 10590134

46. Melikyan GB, Markosyan RM, Hemmati H, Delmedico MK, Lambert DM, Cohen FS. Evidence that the transition of HIV-1 gp41 into a six-helix bundle, not the bundle configuration, induces membrane fusion The Journal of cell biology. 2000; 151(2):413–24. https://doi.org/10.1083/jcb.151.2.413 PMID: 11038187

47. Gallo SA, Clore GM, Louis JM, Bewley CA, Blumenthal R. Temperature-dependent intermediates in HIV-1 envelope glycoprotein-mediated fusion revealed by inhibitors that target N- and C-terminal helical regions of HIV-1 gp41. Biochemistry. 2004; 43(25):8230–3. https://doi.org/10.1021/bi049957v PMID: 15209519

48. Zaitseva E, Zaitsev E, Melikov K, Arakelyan A, Marin M, Villasmil R, et al. Fusion Stage of HIV-1 Entry Depends on Virus-Induced Cell Surface Exposure of Phosphatidylserine. Cell host & microbe. 2017; 22 (1):99–110 e7. https://doi.org/10.1016/j.chom.2017.06.012 PMID: 28704658

49. Amos B, Lotan R. Modulation of lysosomal-associated membrane glycoproteins during retinoic acid-induced embryonal carcinoma cell differentiation. The Journal of biological chemistry. 1990; 265 (31):19192–8. PMID: 2172246

50. Chernomordik L, Leikina E, Cho MS, Zimmerberg J. Control of baculovirus gp64-induced syncytium formation by membrane lipid composition. J Virol. 1995; 69(5):3049–58. https://doi.org/10.1128/JVI.69.5.3049-3058.1995 PMID: 7707532

51. Chernomordik LV, Leikina EA, Zimmerberg J. Lysolipid inhibition of low pH-triggered viral fusion. Biophys J. 1994; 66(2):A6.

52. Melikyan GB, Egelhofer M, von Laer D. Membrane-anchored inhibitory peptides capture human immunodeficiency virus type 1 gp41 conformations that engage the target membrane prior to fusion. J Virol. 2006; 80(7):3249–58. https://doi.org/10.1128/JVI.80.7.3249-3258.2006 PMID: 16537592

53. Chernomordik LV, Frolov VA, Leikina E, Bronk P, Zimmerberg J. The pathway of membrane fusion catalyzed by influenza hemagglutinin: restriction of lipids, hemifusion, and lipidic fusion pore formation. The Journal of cell biology. 1998; 140(6):1369–82. https://doi.org/10.1083/jcb.140.6.1369 PMID: 9508770

54. Chernomordik LV, Kozlov MM. Membrane hemifusion: crossing a chasm in two leaps. Cell. 2005; 123 (3):375–82. https://doi.org/10.1016/j.cell.2005.10.015 PMID: 16269330

55. Cohen FS, Melikyan GB. The energetics of membrane fusion from binding, through hemifusion, pore formation, and pore enlargement. The Journal of membrane biology. 2004; 199(1):1–14. https://doi.org/10.1007/s00232-004-0669-8 PMID: 15366419

56. Earp LJ, Delos SE, Park HE, White JM. The many mechanisms of viral membrane fusion proteins. Curr Top Microbiol Immunol. 2005; 285:25–66. https://doi.org/10.1007/3-540-26764-6_2 PMID: 15609500

57. Melikyan GB, Brener SA, Ok DC, Cohen FS. Inner but not outer membrane leaflets control the transition from glycosylphosphatidylinositol-anchored influenza hemagglutinin-induced hemifusion to full fusion. J Cell Biol. 1997; 136:995–1005. https://doi.org/10.1083/jcb.136.5.995 PMID: 9060465

58. Kozlovsky Y, Chernomordik LV, Kozlov MM. Lipid intermediates in membrane fusion: formation, structure, and decay of hemifusion diaphragm. Biophys J. 2002; 83(5):2634–51. https://doi.org/10.1016/S0006-3495(02)75274-0 PMID: 12414697

59. Markosyan RM, Bates P, Cohen FS, Melikyan GB. A study of low pH-induced refolding of Env of avian sarcoma and leukosis virus into a six-helix bundle. Biophys J. 2004; 87(5):3291–8. https://doi.org/10.1529/biophysj.104.047696 PMID: 15339808

60. Chernomordik LV, Leikina E, Frolov V, Bronk P, Zimmerberg J. An early stage of membrane fusion mediated by the low pH conformation of influenza hemagglutinin depends upon membrane lipids. The Journal of cell biology. 1997; 136(1):81–93. https://doi.org/10.1083/jcb.136.1.81 PMID: 9008705

61. Schoch C, Blumenthal R, Clague MJ. A long-lived state for influenza virus-erythrocyte complexes committed to fusion at neutral pH. FEBS Lett. 1992; 311(3):221–5. https://doi.org/10.1016/0014-5793(92)81107-w PMID: 1397318

62. York J, Dai D, Amberg SM, Nunberg JH. pH-induced activation of arenavirus membrane fusion is antagonized by small-molecule inhibitors. J Virol. 2008; 82(21):10932–9. https://doi.org/10.1128/JVI.01140-08 PMID: 18768973

63. Kobayashi T, Beuchat MH, Chevallier J, Makino A, Mayran N, Escola JM, et al. Separation and characterization of late endosomal membrane domains. The Journal of biological chemistry. 2002; 277(35):32157–64. https://doi.org/10.1074/jbc.M202838200 PMID: 12065580

64. Kobayashi T, Stang E, Fang KS, de Moerloose P, Parton RG, Gruenberg J. A lipid associated with the antiphospholipid syndrome regulates endosome structure and function. Nature. 1998; 392(6672):193–7. https://doi.org/10.1038/32440 PMID: 9515966

65. Kobayashi T, Beuchat MH, Lindsay M, Frias S, Palmiter RD, Sakuraba H, et al. Late endosomal membranes rich in lysobisphosphatidic acid regulate cholesterol transport. Nat Cell Biol. 1999; 1(2):113–8. https://doi.org/10.1038/10084 PMID: 10559883

66. Gallala HD, Sandhoff K. Biological function of the cellular lipid BMP-BMP as a key activator for cholesterol sorting and membrane digestion. Neurochem Res. 2011; 36(9):1594–600. https://doi.org/10.1007/s11064-010-0337-6 PMID: 21136156

67. Hullin-Matsuda F, Luquain-Costaz C, Bouvier J, Delton-Vandenbroucke I. Bis(monoacylglycero)phosphate, a peculiar phospholipid to control the fate of cholesterol: Implications in pathology. Prostaglandins Leukot Essent Fatty Acids. 2009; 81(5–6):313–24. https://doi.org/10.1016/j.plefa.2009.09.006 PMID: 19857945

68. Gruenberg J. Life in the lumen: The multivesicular endosome. Traffic. 2020; 21(1):76–93. https://doi.org/10.1111/tra.12715 PMID: 31854087

69. Roth SL, Whittaker GR. Promotion of vesicular stomatitis virus fusion by the endosome-specific phospholipid bis(monoacylglycero)phosphate (BMP). FEBS Lett. 2011; 585(6):865–9. https://doi.org/10.1016/j.febslet.2011.02.015 PMID: 21333650

70. Markosyan RM, Cohen FS, Melikyan GB. HIV-1 envelope proteins complete their folding into six-helix bundles immediately after fusion pore formation. Mol Biol Cell. 2003; 14(3):926–38. https://doi.org/10.1091/mbc.e02-09-0573 PMID: 12631714

71. Markosyan RM, Cohen FS, Melikyan GB. Time-resolved imaging of HIV-1 Env-mediated lipid and content mixing between a single virion and cell membrane. Molecular biology of the cell. 2005; 16(12):5502–13. https://doi.org/10.1091/mbc.e05-06-0496 PMID: 16195349

72. Cavrois M, De Noronha C, Greene WC. A sensitive and specific enzyme-based assay detecting HIV-1 virion fusion in primary T lymphocytes. Nat Biotechnol. 2002; 20(11):1151–4. https://doi.org/10.1038/nbt745 PMID: 12355096

73. Mobius W, van Donselaar E, Ohno-Iwashita Y, Shimada Y, Heijnen HF, Slot JW, et al. Recycling compartments and the internal vesicles of multivesicular bodies harbor most of the cholesterol found in the endocytic pathway. Traffic. 2003; 4(4):222–31. https://doi.org/10.1034/j.1600-0854.2003.00072.x PMID: 12694561

74. Chevallier J, Chamoun Z, Jiang G, Prestwich G, Sakai N, Matile S, et al. Lysobisphosphatidic acid controls endosomal cholesterol levels. The Journal of biological chemistry. 2008; 283(41):27871–80. https://doi.org/10.1074/jbc.M801463200 PMID: 18644787

75. Wojtanik KM, Liscum L. The transport of low density lipoprotein-derived cholesterol to the plasma membrane is defective in NPC1 cells. The Journal of biological chemistry. 2003; 278(17):14850–6. https://doi.org/10.1074/jbc.M300488200 PMID: 12591922

76. Carette JE, Raaben M, Wong AC, Herbert AS, Obernosterer G, Mulherkar N, et al. Ebola virus entry requires the cholesterol transporter Niemann-Pick C1. Nature. 2011; 477(7364):340–3. https://doi.org/10.1038/nature10348 PMID: 21866103

77. Cote M, Misasi J, Ren T, Bruchez A, Lee K, Filone CM, et al. Small molecule inhibitors reveal Niemann-Pick C1 is essential for Ebola virus infection. Nature. 2011; 477(7364):344–8. https://doi.org/10.1038/nature10380 PMID: 21866101

78. Suddala KC, Lee CC, Meraner P, Marin M, Markosyan RM, Desai TM, et al. Interferon-induced transmembrane protein 3 blocks fusion of sensitive but not resistant viruses by partitioning into virus-carrying endosomes. PLoS Pathog. 2019; 15(1):e1007532. https://doi.org/10.1371/journal.ppat.1007532 PMID: 30640957

79. Brass AL, Huang IC, Benita Y, John SP, Krishnan MN, Feeley EM, et al. The IFITM proteins mediate cellular resistance to influenza A H1N1 virus, West Nile virus, and dengue virus. Cell. 2009; 139 (7):1243–54. https://doi.org/10.1016/j.cell.2009.12.017 PMID: 20064371

80. Melikyan GB, Lin S, Roth MG, Cohen FS. Amino acid sequence requirements of the transmembrane and cytoplasmic domains of influenza virus hemagglutinin for viable membrane fusion. Molecular biology of the cell. 1999; 10(6):1821–36. https://doi.org/10.1091/mbc.10.6.1821 PMID: 10359599

81. Mothes W, Boerger AL, Narayan S, Cunningham JM, Young JA. Retroviral entry mediated by receptor priming and low pH triggering of an envelope glycoprotein. Cell. 2000; 103(4):679–89. https://doi.org/10.1016/s0092-8674(00)00170-7 PMID: 11106737

82. Klewitz C, Klenk HD, ter Meulen J. Amino acids from both N-terminal hydrophobic regions of the Lassa virus envelope glycoprotein GP-2 are critical for pH-dependent membrane fusion and infectivity. The Journal of general virology. 2007; 88(Pt 8):2320–8. https://doi.org/10.1099/vir.0.82950-0 PMID: 17622638

83. Kunz S, Borrow P, Oldstone MB. Receptor structure, binding, and cell entry of arenaviruses. Curr Top Microbiol Immunol. 2002; 262:111–37. https://doi.org/10.1007/978-3-642-56029-3_5 PMID: 11987803

84. Guo X, Steinkuhler J, Marin M, Li X, Lu W, Dimova R, et al. Interferon-Induced Transmembrane Protein 3 Blocks Fusion of Diverse Enveloped Viruses by Altering Mechanical Properties of Cell Membranes. ACS nano. 2021. https://doi.org/10.1021/acsnano.0c10567 PMID: 33656312

85. Matsuo H, Chevallier J, Mayran N, Le Blanc I, Ferguson C, Faure J, et al. Role of LBPA and Alix in multivesicular liposome formation and endosome organization. Science. 2004; 303(5657):531–4. https://doi.org/10.1126/science.1092425 PMID: 14739459

86. Bissig C, Lenoir M, Velluz MC, Kufareva I, Abagyan R, Overduin M, et al. Viral infection controlled by a calcium-dependent lipid-binding module in ALIX. Dev Cell. 2013; 25(4):364–73. https://doi.org/10.1016/j.devcel.2013.04.003 PMID: 23664863

87. Kielian MC, Helenius A. Role of cholesterol in fusion of Semliki Forest virus with membranes. J Virol. 1984; 52(1):281–3. https://doi.org/10.1128/JVI.52.1.281-283.1984 PMID: 6481854

88. Nieva JL, Bron R., Corver J., Wilschut J. Membrane fusion of Semliki Forest Virus requires sphingolipds in the target membrane. EMBO J. 1994; 13(12):2797–804. PMID: 8026464

89. Zaitseva E, Yang S-T, Melikov K, Pourmal S, Chernomordik LV. Dengue Virus Ensures Its Fusion in Late Endosomes Using Compartment-Specific Lipids. PLoS Pathog. 2010; 6(10)(e1001131. https://doi.org/10.1371/journal.ppat.1001131 PMID: 20949067

90. Nour AM, Li Y, Wolenski J, Modis Y. Viral Membrane Fusion and Nucleocapsid Delivery into the Cytoplasm are Distinct Events in Some Flaviviruses. PLoS Pathog. 2013; 9(9):e1003585. https://doi.org/10.1371/journal.ppat.1003585 PMID: 24039574

91. Razinkov VI, Cohen FS. Sterols and sphingolipids strongly affect the growth of fusion pores induced by the hemagglutinin of influenza virus. Biochemistry. 2000; 39(44):13462–8. https://doi.org/10.1021/bi0012078 PMID: 11063582

92. Matos PM, Marin M, Ahn B, Lam W, Santos NC, Melikyan GB. Anionic lipids are required for vesicular stomatitis virus G protein-mediated single particle fusion with supported lipid bilayers. The Journal of biological chemistry. 2013; 288(18):12416–25. https://doi.org/10.1074/jbc.M113.462028 PMID: 23493401

93. Marin M, Kushnareva Y, Mason CS, Chanda SK, Melikyan GB. HIV-1 Fusion with CD4+ T cells Is Promoted by Proteins Involved in Endocytosis and Intracellular Membrane Trafficking. Viruses. 2019; 11 (2). https://doi.org/10.3390/v11020100 PMID: 30691001

94. He J, Choe S, Walker R, Di Marzio P, Morgan DO, Landau NR. Human immunodeficiency virus type 1 viral protein R (Vpr) arrests cells in the G2 phase of the cell cycle by inhibiting p34cdc2 activity. J Virol. 1995; 69(11):6705–11. https://doi.org/10.1128/JVI.69.11.6705-6711.1995 PMID: 7474080

95. Hammonds J, Chen X, Zhang X, Lee F, Spearman P. Advances in methods for the production, purification, and characterization of HIV-1 Gag-Env pseudovirion vaccines. Vaccine. 2007; 25(47):8036–48. https://doi.org/10.1016/j.vaccine.2007.09.016 PMID: 17936444